

A NEW MIXED FINITE-ELEMENT METHOD FOR THE BIHARMONIC PROBLEM*

PATRICK E. FARRELL[†], ABDALAZIZ HAMDAN[‡], AND SCOTT P. MACLACHLAN[‡]

Abstract. Fourth-order differential equations play an important role in many applications in science and engineering. In this paper, we present a three-field mixed finite-element formulation for fourth-order problems, with a focus on the effective treatment of the different boundary conditions that arise naturally in a variational formulation. Our formulation is based on introducing the gradient of the solution as an explicit variable, constrained using a Lagrange multiplier. The essential boundary conditions are enforced weakly, using Nitsche’s method where required. As a result, the problem is rewritten as a saddle-point system, requiring analysis of the resulting finite-element discretization and the construction of optimal linear solvers. Here, we discuss the analysis of the well-posedness and accuracy of the finite-element formulation. Moreover, we develop monolithic multigrid solvers for the resulting linear systems. Two and three-dimensional numerical results are presented to demonstrate the accuracy of the discretization and efficiency of the multigrid solvers proposed.

Key words. Mixed Finite-Element Methods, Biharmonic Equation, Multigrid Methods, Saddle-Point Problems

AMS subject classifications. 65N30, 65N55, 65F08

1. Introduction. Fourth-order differential operators often appear in mathematical models of thin films and plates [27, 44, 49], and pose significant challenges in numerical simulation in comparison to equations governed by more familiar second-order operators. Similar challenges arise from modeling equilibrium states of smectic A liquid crystals (LCs), which correspond to minimizers of a given energy functional. For example, the Pevnyi, Selinger, and Sluckin energy functional for smectic A liquid crystals is given by [49]:

$$(1.1) \quad I(u, \vec{n}) = \int_{\Omega} \frac{a}{2} u^2 + \frac{b}{3} u^3 + \frac{c}{4} u^4 + B[(\partial_i \partial_j + q^2 n_i n_j)u]^2 + \frac{K}{2} (\partial_i n_j)^2,$$

where $\Omega \subset \mathbb{R}^d$, $d \in \{2, 3\}$, a, b, q, B , and K are positive real-valued constants determined by the experiment and material under consideration, $\vec{n} : \Omega \rightarrow \mathbb{R}^d$ is a unit vector field called the director, and $u : \Omega \rightarrow \mathbb{R}$ is the smectic order parameter representing the density variation of the LC. This energy is to be minimized subject to the constraint that $\vec{n} \cdot \vec{n} = 1$ pointwise almost everywhere. When enforcing this constraint with a Lagrange multiplier, the Euler–Lagrange equations for (1.1) lead to a coupled system of PDEs, with a fourth-order operator applied to u , a second-order operator acting on \vec{n} , and an algebraic constraint.

Motivated by such examples, several families of finite-element methods have been developed to approximate solutions of PDEs with fourth-order terms. In this work, we consider minimization of a simplified form of the energy (1.1) with suitable boundary conditions, given in variational form as

$$(1.2) \quad \min_{v \in H^2(\Omega)} \frac{1}{2} \int_{\Omega} (\Delta v)^2 + c_0 \nabla v \cdot \nabla v + c_1 v^2 - \int_{\Omega} f v,$$

*Submitted to the editors DATE.

Funding: The work of AH and SM was partially supported by an NSERC discovery grant. The work of PEF is supported by EPSRC grants EP/R029423/1 and EP/V001493/1.

[†]Mathematical Institute, University of Oxford, Oxford, UK (patrick.farrell@maths.ox.ac.uk).

[‡]Department of Mathematics and Statistics, Memorial University of Newfoundland, St. John’s, NL, Canada (ahamdan@mun.ca, smaclachlan@mun.ca).

with nonnegative constants c_0 and c_1 . While the variational formulation in (1.1) is written in terms of the Hessian operator, here we consider the classical fourth-order biharmonic (Laplacian squared) and will consider the Hessian problem in future work. Sufficiently smooth extremizers of (1.2) must satisfy its Euler–Lagrange equations, which yield a fourth-order problem,

$$(1.3) \quad \Delta^2 u - c_0 \Delta u + c_1 u = f.$$

We consider three-field mixed formulations for this fourth-order problem, with a particular focus on the treatment of the boundary conditions that arise naturally from the transition from the variational to strong forms. These formulations introduce the gradient of the solution as an explicit variable constrained using a Lagrange multiplier. Our approach is general in the sense that we are able to use elements of order k , $k + 1$, and $k + 1$ for the solution, its gradient, and the Lagrange multiplier respectively, where k can be as large as the smoothness of the solution allows. The existence and uniqueness proofs are not complicated. A drawback here is our formulation provides suboptimal convergence for some boundary conditions, as discussed below.

If $c_0 = c_1 = 0$, then (1.2) represents the classical biharmonic equation. Many different types of finite-element methods have been considered in this context. Conforming methods, in which the finite-dimensional space is a subspace of the Sobolev space $H^2(\Omega)$, rely on the use of complicated basis functions. These require a high number of degrees of freedom per element, especially in three dimensions. Moreover, the elements are typically not affine equivalent; i.e. the basis functions cannot be mapped to each element using a reference element in the standard way, and more complicated approaches are needed [24, 36, 38]. In order to avoid the use of such C^1 elements, other types of finite elements can be used, leading to nonconforming methods in which the finite-element space is not a subspace of $H^2(\Omega)$, such as Morley and cubic Hermite elements [21, 24, 54]. These elements are also complex to implement and require analysis of the consistency error, which sometimes implies suboptimal convergence when the consistency error is larger than the interpolation error of the element [55].

C^0 interior penalty methods (C0IP) can also be used for fourth-order problems, where the continuity of the function derivatives are weakly enforced using stabilization terms on interior edges [10, 20, 22]. Brenner, Sung, and Zhang [22] solved the problem $\Delta^2 u - \nabla \cdot (\beta(x) \nabla u) = f$, where $\beta(x)$ is a nonnegative C^1 function. Their approach is to find $u \in CG_k(\Omega, \tau_h)$, $k \geq 2$, that satisfies the system

$$(1.4) \quad a_h(u, \phi) + b_h(u, \phi) + \gamma c_h(u, \phi) = \langle f, \phi \rangle, \quad \forall \phi \in CG_k(\Omega, \tau_h),$$

where $\gamma > 0$ is a penalty parameter, $CG_k(\Omega, \tau_h)$ is the space of continuous Lagrange elements of degree k on a triangulation τ_h of the domain Ω , and

$$(1.5) \quad a_h(u, \phi) = \sum_{T \in \tau_h} \int_T (\nabla \nabla u : \nabla \nabla \phi + \beta(x) \nabla u \cdot \nabla \phi),$$

$$(1.6) \quad b_h(u, \phi) = \sum_{e \in \epsilon_h} \int_e \left\{ \frac{\partial^2 u}{\partial^2 n} \right\} \left[\frac{\partial \phi}{\partial n} \right] + \sum_{e \in \epsilon_h} \int_e \left\{ \frac{\partial^2 \phi}{\partial^2 n} \right\} \left[\frac{\partial u}{\partial n} \right],$$

$$(1.7) \quad c_h(u, \phi) = \sum_{e \in \epsilon_h} \frac{1}{|e|} \int_e \left[\frac{\partial u}{\partial n} \right] \left[\frac{\partial \phi}{\partial n} \right],$$

where $\{\frac{\partial u}{\partial n}\}$ and $[\frac{\partial \phi}{\partial n}]$ denote the standard average and jump on each edge. Here τ_h is the set of cells in a mesh and ϵ_h is the set of edges. While COIP methods have advantages like enabling the use of simple Lagrange elements, and the ability to use arbitrarily high-order elements [22], they also have some disadvantages. The weak forms are more complicated than those used for classical conforming and nonconforming methods. Moreover, the need for the penalty parameter is also a drawback, as it is sometimes not trivial to decide how large this parameter must be to achieve stability, especially as parameters in the PDE are varied [47]. Similarly, discontinuous Galerkin approaches can also be applied to this problem [11], augmenting the forms in (1.4) to account for basis functions that do not enforce C^0 continuity across elements. These share the disadvantages of COIP methods, while requiring more degrees of freedom than C^0 approaches.

Another attractive option to avoid using H^2 -conforming methods is mixed finite-element methods, in which the gradient or the Laplacian of the solution are approximated in addition to the solution itself [13–15, 23, 24, 40, 42]. A natural classification of such mixed finite-element methods is based on how many functions (fields) are directly approximated. Given clamped boundary conditions, i.e., the unknown function and its gradient are given on the boundary, two functions were approximated in [23, 24, 42], which are the unknown function u and its gradient or Laplacian. In [24], the biharmonic problem is rewritten as a coupled system of Poisson equations, in which the unknown and its Laplacian are both directly approximated. In [42], the 2D biharmonic problem is approximated by minimizing

$$J(u, \vec{v}) = \frac{1}{2} \|\nabla \vec{v}\|_0^2 + \frac{1}{2\epsilon} \|\rho_0(\vec{v} - \nabla u)\|_0^2 - \langle f, u \rangle, \quad \text{for } 0 < \epsilon \leq ch^2,$$

where ρ_0 is the orthogonal projection from $[L^2(\Omega)]^2$ to the space of piecewise constant functions, and the functions u and \vec{v} are approximated using bilinear elements on a rectangular mesh. An error analysis of this method requires the solution to be at least in $H^{4.73}(\Omega)$ [34]. A similar approach solves the d -dimensional biharmonic problem, replacing the L^2 projection onto piecewise constant functions with that onto the space of multilinear vector-valued functions whose i^{th} component is independent of x_i [23]. This approach requires less regularity on the solution, $u \in H^4(\Omega)$, than was required in [42]. These approaches only treat clamped boundary conditions.

A second class of mixed finite-element methods is that of four-field formulations, in which u , ∇u , $\nabla^2 u$, and $\nabla \cdot (\nabla^2 u)$ are directly approximated. In [40], a mixed formulation approximating these fields and its stability in $H_0^1(\Omega) \times [H_0^1(\Omega)]^2 \times \mathbf{L}_{\text{sym}}^2(\Omega) \times H^{-1}(\text{div}; \Omega)$ is discussed, where $\mathbf{L}_{\text{sym}}^2(\Omega)$ is the space of 2×2 symmetric tensors with components in $L^2(\Omega)$, and $H^{-1}(\text{div}; \Omega)$ is the dual space of $H_0(\text{rot}; \Omega)$. A similar approach with different function spaces is given in [15]. This approach, focused on the discrete level, finds $(u_h, \vec{q}_h, \vec{z}_h, \vec{\sigma}_h) \in DG_k(\Omega, \tau_h) \times [DG_k(\Omega, \tau_h)]^2 \times \mathbf{RT}_k(\Omega, \tau_h) \times \mathbf{RT}_k(\Omega, \tau_h) \subset L^2(\Omega) \times [L^2(\Omega)]^2 \times \mathbf{H}(\text{div}; \Omega) \times H(\text{div}; \Omega)$, where $u_h, \vec{q}_h, \vec{z}_h$, and $\vec{\sigma}_h$ are approximations of $u, \nabla u, \nabla^2 u$, and $\nabla \cdot (\nabla^2 u)$ respectively, and $\vec{y} \in \mathbf{H}(\text{div}; \Omega)$ means that each row of the tensor \vec{y} belongs to $H(\text{div}; \Omega)$. Here $DG_k(\Omega, \tau_h)$ and $\mathbf{RT}_k(\Omega, \tau_h)$ denote the discontinuous Lagrange and Raviart–Thomas approximation spaces of order k , respectively, with $\mathbf{RT}_k(\Omega, \tau_h)$ denoting tensor-valued functions with rows in $\mathbf{RT}_k(\Omega, \tau_h)$. However, these four-field formulations lead to discretizations with large numbers of degrees of freedom, posing difficulties in the development of efficient linear solvers.

The third class of mixed finite-element methods is that of three-field formulations

[13]. The unknowns here are the function, its gradient, and a Lagrange multiplier. Assuming again homogeneous clamped boundary conditions, these lead to finding the saddle-point $(u, \vec{v}, \vec{\alpha}) \in H_0^1(\Omega) \times H_0(\text{div}; \Omega) \times M$ of the Lagrangian functional

$$(1.8) \quad \mathcal{L}((u, \vec{v}), \vec{\alpha}) = \frac{1}{2} \|\nabla \cdot \vec{v}\|_0^2 + \int_{\Omega} \vec{\alpha} \cdot (\vec{v} - \nabla u) - \int_{\Omega} f u$$

where $M = \{\vec{\alpha} \in H_0(\text{div}; \Omega) \mid \nabla \cdot \vec{\alpha} \in H^{-1}(\Omega)\}$. Here, $H_0(\text{div}; \Omega) := \{\vec{v} \in H(\text{div}; \Omega) \mid \vec{v} \cdot \vec{n} = 0 \text{ on } \partial\Omega\}$. At the discrete level, the method in [13] finds $(u_h, \vec{v}_h, \vec{\alpha}_{2h}) \in CG_1(\Omega, \tau_h) \times RT_1(\Omega, \tau_h) \times DG_0(\Omega, \tau_{2h})$, where the Lagrange multiplier $\vec{\alpha}_{2h}$ is constructed in τ_{2h} to guarantee well-posedness at the discrete level and to achieve an optimal error estimate. Again, this approach only treats clamped boundary conditions, and requires the use of different meshes in the discretization. Moreover, it is not mentioned if the discretization can be generalized to higher orders. Here, we propose a similar three-field formulation, but treating the generalized problem in (1.3) with more general boundary conditions, and using different discretization spaces of arbitrarily high degree. Unlike conforming methods, our approach works effectively in both two and three dimensions.

Strongly imposing essential boundary conditions with some finite-element basis functions is difficult [36]. In addition, it can, sometimes, negatively affect properties of the finite-element method, such as its stability and accuracy [33, 35]. Weakly imposing the boundary conditions via a penalty method [8, 9] may help. An attractive family of penalty methods are the Nitsche-type methods [48] for which optimal convergence can be achieved. Applications of Nitsche's method to second-order PDEs can be found in [30, 33, 35]. Moreover, Nitsche-type penalty methods have been used to impose essential boundary conditions for some discretizations of the biharmonic and other fourth-order problems [16, 26, 36]. While we are able to impose a variety of boundary conditions directly in our variational formulation, we utilize Nitsche-type penalty methods for a particular case where strong enforcement of the boundary conditions leads to problems establishing inf-sup stability of the discretization.

At the discrete level, the resulting linear system of our three-field formulation is a saddle point system [17], of the form

$$\begin{bmatrix} A & B^T \\ B & 0 \end{bmatrix} \begin{bmatrix} U \\ \alpha \end{bmatrix} = \begin{bmatrix} f \\ g \end{bmatrix}$$

where U represents discrete degrees of freedom associated with both u and \vec{v} , while α represents discrete degrees of freedom associated with $\vec{\alpha}$, leading to matrices $A \in \mathbb{R}^{n \times n}$, $B \in \mathbb{R}^{m \times n}$ and the zero matrix $0 \in \mathbb{R}^{m \times m}$. In our formulation, A will be symmetric and positive semi-definite except for the case where we enforce the boundary conditions weakly through Nitsche's method. This kind of problem appears in many areas of computational science and engineering [17]. For discretized PDEs, the condition number of such systems usually grows like h^{-k} for $k > 0$, resulting in increasingly ill-conditioned systems as the mesh size, h , goes to zero. This growth of the condition number leads to slow convergence of unpreconditioned Krylov methods. Therefore, we employ preconditioning in order to develop a mesh-independent algorithm to solve these systems. Two common families of preconditioners can be considered here; block factorization [25, 29, 45] and monolithic multigrid preconditioners [1–3, 53]. In this work, we propose a mixed finite-element discretization framework that allows us to leverage effective monolithic multigrid solvers for saddle-point systems [2, 3, 28].

This paper is organized as follows. In Section 2, a brief summary is given of the Sobolev and finite-element spaces employed. The weak forms, uniqueness of solutions

at the continuum and discrete levels, and an error analysis are presented in Sections 3 and 4. The monolithic multigrid preconditioner and the details of the linear solver are presented in Section 5. Finally, numerical experiments showing the accuracy of the finite-element method and the effectiveness of the linear solver are given in Section 6.

2. Background. On a simplex $T \in \tau_h$, all degrees of freedom of the discontinuous Lagrange $DG_k(\Omega, \tau_h)$ element are considered to be internal; i.e., global continuity is not imposed by these elements [38]. In contrast, the continuous Lagrange $CG_k(\Omega, \tau_h)$ elements possess full C^0 continuity across element edges. Here, we primarily make use of $DG_k(\Omega, \tau_h)$ approximations of functions in $L^2(\Omega)$. A standard approximation result for these elements is stated next.

THEOREM 2.1. [18, 19, 38] *Let $I_h^k : H^{k+1}(\Omega) \rightarrow DG_k(\Omega, \tau_h)$, $\Pi_h^k : [H^{k+1}(\Omega)]^d \rightarrow RT_k(\Omega, \tau_h)$, and $L_h^k : [H^{k+1}(\Omega)]^d \rightarrow [CG_k(\Omega, \tau_h)]^d$ be the finite-element interpolation operators. Then there exist constants \tilde{c} , c , and \hat{c} , such that for any $u \in H^{k+1}(\Omega)$ and $\vec{v} \in [H^{k+1}(\Omega)]^d$,*

$$(2.1) \quad \|u - I_h^k u\|_0 \leq \tilde{c} h^{k+1} |u|_{k+1}, \quad \forall k \geq 0,$$

$$(2.2) \quad \|\vec{v} - \Pi_h^k \vec{v}\|_{\text{div}} \leq c h^k |\vec{v}|_{k+1}, \quad \forall k > 0,$$

and

$$(2.3) \quad \|(\vec{v} - L_h^k \vec{v})\|_1 \leq \hat{c} h^k |\vec{v}|_{k+1}, \quad \forall k > 0.$$

As we will make use of a mixed formulation, our proofs will be aided by recalling a standard result for mixed formulations of the Poisson problem as follows.

LEMMA 2.2. [18, 46] *Given $u \in L^2(\Omega)$, define ϕ as the solution of*

$$\begin{aligned} \Delta \phi &= u \text{ in } \Omega, \\ \phi &= 0 \text{ on } \Gamma_D, \text{ and } \nabla u \cdot \vec{n} = 0 \text{ on } \Gamma_N, \end{aligned}$$

where Γ_D is nonempty. Let $V = H_{\Gamma_N}(\text{div}; \Omega)$ and $Q = L^2(\Omega)$. The mixed formulation to find $(\vec{\alpha}, \phi) \in V \times Q$ such that

$$(2.4) \quad \int_{\Omega} \eta \nabla \cdot \vec{\alpha} = \int_{\Omega} u \eta, \quad \forall \eta \in Q,$$

$$(2.5) \quad \int_{\Omega} \vec{\alpha} \cdot \vec{\beta} + \phi \nabla \cdot \vec{\beta} = 0, \quad \forall \vec{\beta} \in V,$$

is well-posed and, moreover, $\|\vec{\alpha}\|_{\text{div}}^2 + \|\phi\|_0^2 \leq \Lambda \|u\|_0^2$, where Λ is a positive constant that depends on the constants of coercivity, continuity, and the inf-sup conditions.

Remark 2.3. The result above is also true at the discrete level, for $u \in DG_k(\Omega, \tau_h)$ and $(V, Q) = RT_{k+1}^{\Gamma_N}(\Omega, \tau_h) \times DG_k(\Omega, \tau_h)$, with $RT_{k+1}^{\Gamma_N}(\Omega, \tau_h) = \{\vec{v} \in RT_{k+1}(\Omega, \tau_h) | \vec{v} \cdot \vec{n} = 0 \text{ on } \Gamma_N\}$. ■

Remark 2.4. The choice of $\eta = u$ in Equation (2.4) implies that $\|u\|_0^2 = \int_{\Omega} u \nabla \cdot \vec{\alpha}$.

An important property of our discretization is that it benefits from the usual mimetic relationships between $RT_{k+1}(\Omega, \tau_h)$ and $DG_k(\Omega, \tau_h)$, summarized in the following results.

LEMMA 2.5. [5, 7] *The Helmholtz decomposition of $RT_{k+1}(\Omega, \tau_h)$ is*

$$(2.6) \quad RT_{k+1}(\Omega, \tau_h) = \left(\nabla \times V_h \right) \oplus \left(\text{grad}_h DG_k(\Omega, \tau_h) \right),$$

where grad_h is the discrete gradient operator, $\text{grad}_h : DG_k(\Omega, \tau_h) \rightarrow RT_{k+1}(\Omega, \tau_h)$, such that

$$\int_{\Omega} \text{grad}_h u \cdot \vec{v} = - \int_{\Omega} u \nabla \cdot \vec{v}, \quad \forall \vec{v} \in RT_{k+1}(\Omega, \tau_h).$$

For $d = 2$, $\nabla \times = \begin{bmatrix} -\frac{\partial}{\partial y} \\ \frac{\partial}{\partial x} \end{bmatrix}$ and $V_h = CG_{k+1}(\Omega, \tau_h)$, while $V_h = N_{k+1}^1(\Omega, \tau_h)$ for $d = 3$, where $N_{k+1}^1(\Omega, \tau_h)$ is the Nédélec element of the first kind of order $k + 1$.

Remark 2.6. [18, 38] $\forall \vec{v} \in RT_{k+1}(\Omega, \tau_h)$, we have $\nabla \cdot \vec{v} \in DG_k(\Omega, \tau_h)$.

While we largely make use of the standard Sobolev norms, we will use the “strengthened” norm,

$$\|v\|_{\text{div}, \Gamma}^2 = \|v\|_{\text{div}}^2 + \|\vec{v} \cdot \vec{n}\|_{0, \Gamma}^2,$$

where $\Gamma \subset \partial\Omega$ (to be specified later), and

$$\|\vec{v} \cdot \vec{n}\|_{0, \Gamma}^2 = \int_{\Gamma} |\vec{v} \cdot \vec{n}|^2.$$

Note that $\forall \vec{v} \in H_0(\text{div}; \Omega)$, $\|\vec{v}\|_{\text{div}} = \|\vec{v}\|_{\text{div}, \Gamma}$. For these norms, the inverse trace inequality below is a useful result.

THEOREM 2.7. [51, 56] *Let τ_h be a triangular mesh of $\Omega \subset \mathbb{R}^2$. Then, for all $T \in \tau_h$ and all $u \in DG_k(T)$,*

$$(2.7) \quad \|u\|_{0, \partial T}^2 \leq \frac{(k+1)(k+2) \text{ Perimeter length } (T)}{2 \text{ Area}(T)} \|u\|_{0, T}^2,$$

where $\|u\|_{0, \partial T}^2$ is defined as

$$(2.8) \quad \|u\|_{0, \partial T}^2 = \int_{\partial T} u^2.$$

COROLLARY 2.8. *Consider a triangulation τ_h of the domain $\Omega \subset \mathbb{R}^2$, and let $\partial\tau_h := \{T \in \tau_h \mid \partial T \cap \partial\Omega \neq \emptyset\}$. Then,*

$$\begin{aligned} \forall u_h \in DG_k(\Omega, \tau_h), \|u_h\|_{0, \partial\Omega}^2 &\leq \gamma_1(k, \tau_h) \|u_h\|_0^2 \\ \forall \vec{v}_h \in RT_{k+1}(\Omega, \tau_h), \|\vec{v}_h \cdot \vec{n}\|_{0, \partial\Omega}^2 &\leq \gamma_2(k, \tau_h) \|\vec{v}_h\|_0^2, \end{aligned}$$

where

$$(2.9) \quad \gamma_1(k, \tau_h) = \max_{T \in \partial\tau_h} \frac{(k+1)(k+2) \text{ Perimeter length } (T)}{2 \text{ Area}(T)},$$

and

$$(2.10) \quad \gamma_2(k, \tau_h) = \max_{T \in \partial\tau_h} \frac{(k+2)(k+3) \text{ Perimeter length } (T)}{2 \text{ Area}(T)}.$$

Proof. Summing (2.7) over $T \in \partial\tau_h$ and using the facts that

$$\|u_h\|_{0, \partial\Omega}^2 \leq \sum_{T \in \partial\tau_h} \|u_h\|_{0, \partial T}^2, \quad \text{and} \quad \sum_{T \in \partial\tau_h} \|u\|_{0, T}^2 \leq \|u\|_0^2$$

completes the proof for $u_h \in DG_k(\Omega, \tau_h)$. Note that the result also holds for the normal component of $\vec{v}_h \in RT_{k+1}(\Omega, \tau_h) \subset [DG_{k+1}(\Omega, \tau_h)]^2$. \square

While the ratio between a triangle's perimeter and its area can be arbitrarily large, the terms $\gamma_1(k, \tau_h)$ and $\gamma_2(k, \tau_h)$ are bounded when we consider quasi-uniform families of meshes [21, Definition 4.4.13], where the perimeter of each triangle is bounded above by $\mathcal{O}(h)$ and the area is bounded below by $\mathcal{O}(h^2)$. This naturally leads to an approximation property for the trace norm. These results will be useful in the analysis of the Nitsche boundary integrals.

COROLLARY 2.9. *Let $\{\tau_h\}$, $0 < h \leq 1$ be a family of quasiuniform meshes of the domain $\Omega \subset \mathbb{R}^2$. Then, $\exists C_\Omega > 0$ such that for any τ_h in the family,*

$$\begin{aligned} \forall u_h \in DG_k(\Omega, \tau_h), \|u_h\|_{0, \partial\Omega}^2 &\leq \frac{\gamma_1(k)}{h} \|u_h\|_0^2 \\ \forall \vec{v}_h \in RT_{k+1}(\Omega, \tau_h), \|\vec{v}_h \cdot \vec{n}\|_{0, \partial\Omega}^2 &\leq \frac{\gamma_2(k)}{h} \|\vec{v}_h\|_0^2, \end{aligned}$$

where

$$(2.11) \quad \gamma_1(k) = h \max_{T \in \partial\tau_h} \frac{(k+1)(k+2) \text{ Perimeter length}(T)}{2 \text{ Area}(T)} \leq C_\Omega (k+1)(k+2),$$

and

$$(2.12) \quad \gamma_2(k) = h \max_{T \in \partial\tau_h} \frac{(k+2)(k+3) \text{ Perimeter length}(T)}{2 \text{ Area}(T)} \leq C_\Omega (k+2)(k+3).$$

Proof. From the definition of a quasi-uniform family of meshes, we have that

$$\begin{aligned} \text{Perimeter length}(T) &\leq 3 \text{diam}(T) \leq 3h \text{diam}(\Omega), \\ \text{Area}(T) &\geq \text{Area}(B_T) = \frac{\pi}{4} (\text{diam}(B_T))^2 \geq \frac{\pi}{4} (\rho h \text{diam}(\Omega))^2, \end{aligned}$$

where B_T is the incircle of T and ρ is the constant from the definition of quasi-uniformity. \square

COROLLARY 2.10. *Let $\{\tau_h\}$, $0 < h \leq 1$ be a family of quasiuniform meshes of the domain $\Omega \subset \mathbb{R}^2$. Let $\Pi_h^{k+1} : [H^{k+2}(\Omega)]^2 \rightarrow RT_{k+1}(\Omega, \tau_h)$ and $L_h^{k+1} : [H^{k+2}(\Omega)]^2 \rightarrow [CG_{k+1}(\Omega, \tau_h)]^2$ be the finite-element interpolation operators and let $\vec{v} \in [H^{k+2}(\Omega)]^2$. Then, there exists a constant, λ , such that*

$$\|(\vec{v} - \Pi_h^{k+1} \vec{v}) \cdot \vec{n}\|_{0, \partial\Omega} \leq \lambda h^{k+1/2} |\vec{v}|_{k+2}.$$

Proof. Applying the triangle inequality,

$$\|(\vec{v} - \Pi_h^{k+1} \vec{v}) \cdot \vec{n}\|_{0, \partial\Omega} \leq \|(\vec{v} - L_h^{k+1} \vec{v}) \cdot \vec{n}\|_{0, \partial\Omega} + \|(L_h^{k+1} \vec{v} - \Pi_h^{k+1} \vec{v}) \cdot \vec{n}\|_{0, \partial\Omega}.$$

Note that the vector-valued function $\vec{v} - L_h^{k+1} \vec{v} \in [H^1(\Omega)]^2$, and therefore, we use the trace theorem [32, Theorem 1.5.1.10],

$$\|(\vec{v} - L_h^{k+1} \vec{v}) \cdot \vec{n}\|_{0, \partial\Omega} \leq K \|\vec{v} - L_h^{k+1} \vec{v}\|_1,$$

where K is a positive constant independent of h . Also, $L_h^{k+1} \vec{v} - \Pi_h^{k+1} \vec{v} \in RT_{k+2}(\tau_h, \Omega)$. Applying Theorem 2.1 and Corollary 2.9,

$$\begin{aligned}
\|(\vec{v} - \Pi_h^{k+1}\vec{v}) \cdot \vec{n}\|_{0,\partial\Omega} &\leq K\|\vec{v} - L_h^{k+1}\vec{v}\|_1 + \|L_h^{k+1}\vec{v} - \Pi_h^{k+1}\vec{v}\|_{0,\partial\Omega} \\
&\leq K\hat{c}h^{k+1}|\vec{v}|_{k+2} + \frac{\eta}{\sqrt{h}}\|L_h^{k+1}\vec{v} - \Pi_h^{k+1}\vec{v}\|_0 \\
&\leq K\hat{c}h^{k+1}|\vec{v}|_{k+2} + \frac{\eta}{\sqrt{h}}(\|L_h^{k+1}\vec{v} - \vec{v}\|_0 + \|\vec{v} - \Pi_h^{k+1}\vec{v}\|_0) \\
&\leq K\hat{c}h^{k+1}|\vec{v}|_{k+2} + \frac{\eta}{\sqrt{h}}(c + \hat{c})h^{k+1}|\vec{v}|_{k+2}
\end{aligned}$$

where $\eta = \sqrt{C_\Omega(k+3)(k+4)}$, the constants c , \hat{c} and C_Ω are defined in Theorem 2.1 and Corollary 2.9. The choice $\lambda = K\hat{c} + (c + \hat{c})\eta$ completes the proof. \square

Remark 2.11. While the analysis above focuses on the case of two-dimensional domains (primarily in quantifying the constants in the inverse-trace inequalities), it is readily extended to three dimensions [56]. Let τ_h be a tetrahedral mesh of $\Omega \subset \mathbb{R}^3$. Then, for an element $T \in \tau_h \subset \mathbb{R}^3$ and all $u \in DG_k(T)$,

$$(2.13) \quad \|u\|_{0,\partial T}^2 \leq \frac{(k+1)(k+3) \text{ Surface area}(T)}{3 \text{ Volume}(T)} \|u\|_{0,T}^2,$$

from here, results analogous to Corollaries 2.8 to 2.10 can be derived noting that on a quasi-uniform mesh in $3D$, $\frac{\text{Surface area}(T)}{\text{Volume}(T)}$ is still bounded by some $\frac{C_\Omega}{h}$.

3. Continuum Analysis. Consider the fourth-order problem from (1.3) with suitable boundary conditions (discussed below),

$$(3.1) \quad \Delta^2 u - c_0 \Delta u + c_1 u = f \text{ in } \Omega,$$

where $\Omega \subset \mathbb{R}^d$ is a bounded polygonal or polyhedral domain with outward pointing normal \vec{n} , and c_0 and c_1 are nonnegative constants. Define $V = \{v \in H^1(\Omega) \mid \Delta v \in L^2(\Omega)\}$, and its dual space V^* . Assume that $u \in V$, and $f \in V^*$ satisfy (3.1). Then given any $v \in V$, it follows from integration by parts that

$$(3.2) \quad \int_\Omega f v = a(u, v) + \int_{\partial\Omega} v(\nabla \Delta u - c_0 \nabla u) \cdot \vec{n} - \int_{\partial\Omega} \Delta u \nabla v \cdot \vec{n},$$

where the bilinear form $a(u, v)$ is defined as

$$(3.3) \quad a(u, v) = \int_\Omega \Delta u \Delta v + c_0 \nabla u \cdot \nabla v + c_1 u v.$$

Since (3.1) is a fourth-order problem, we require two boundary conditions on any segment of $\partial\Omega$. Here, we focus on the boundary conditions that arise naturally from the variational formulation in (3.2):

$$(3.4) \quad u = g_0, \quad \Delta u = g_1, \quad \text{on } \Gamma_0,$$

$$(3.5) \quad u = g_0, \quad \frac{\partial u}{\partial n} = g_2, \quad \text{on } \Gamma_1,$$

$$(3.6) \quad \frac{\partial(\Delta u - c_0 u)}{\partial n} = g_3, \quad \Delta u = g_1, \quad \text{on } \Gamma_2,$$

$$(3.7) \quad \frac{\partial(\Delta u - c_0 u)}{\partial n} = g_3, \quad \frac{\partial u}{\partial n} = g_2, \quad \text{on } \Gamma_3,$$

where g_0, g_1, g_2 and g_3 are sufficiently smooth functions. We note that the commonly-considered case of clamped boundary conditions corresponds to Γ_1 in this classification. Under suitable assumptions on c_0 and c_1 , we can prove a variety of results on the well-posedness of (3.2) in the standard Hilbert space setting.

LEMMA 3.1. Equip $V = \{u \in H^1(\Omega) \mid \Delta u \in L^2(\Omega)\}$ with the inner product

$$(u, v) = \int_{\Omega} uv + \nabla u \cdot \nabla v + \Delta u \Delta v, \quad \forall u, v \in V.$$

The normed space $(V, \|\cdot\|_V)$ is a Hilbert space.

THEOREM 3.2. Assume that $\partial\Omega = \Gamma_0 \cup \Gamma_1 \cup \Gamma_2 \cup \Gamma_3$ with $\Gamma_i \cap \Gamma_j = \emptyset$ for $i \neq j$. Then Problem (3.2) is well-posed for $c_0, c_1 > 0$.

Proof. Define $V_0 = \{v \in V \mid v = 0 \text{ on } \Gamma_0 \cup \Gamma_1 \text{ and } \frac{\partial v}{\partial n} = 0 \text{ on } \Gamma_1 \cup \Gamma_3\}$. Using standard techniques (cf. [31]), we transform the inhomogeneous boundary conditions (3.4)-(3.7) into homogeneous ones. The resulting weak form is to find $u - u_1 \in V_0$ such that

$$(3.8) \quad a(u - u_1, v) = F(v), \quad \forall v \in V_0,$$

where the bilinear form a is defined in (3.3), u_1 is a known function that satisfies $u_1 = g_0$ on $\Gamma_0 \cup \Gamma_1$ and $\frac{\partial u_1}{\partial n} = g_2$ on $\Gamma_1 \cup \Gamma_3$, and $F(v)$ is defined as

$$(3.9) \quad F(v) = \int_{\Omega} f v - \int_{\Gamma_2 \cup \Gamma_3} g_3 v + \int_{\Gamma_0 \cup \Gamma_2} g_1 \frac{\partial v}{\partial n} - a(u_1, v).$$

The bilinear form a is symmetric, continuous and coercive on V_0 , with continuity constant $\lambda_1 = \max\{1, c_0, c_1\}$ and coercivity constant $\lambda_0 = \min\{1, c_0, c_1\}$, and the linear form F is continuous. Thus, Problem (3.8) is well-posed by the Lax-Milgram Theorem, and thus Problem (3.2) is also. \square

COROLLARY 3.3. Problem 3.2 with $c_0 = 0$ and $c_1 > 0$ is well-posed when $\partial\Omega = \Gamma_0 \cup \Gamma_1 \cup \Gamma_3$ with $\Gamma_i \cap \Gamma_j = \emptyset$ for $i \neq j$.

Proof. The weak form in this case is identical to that given in (3.8), but we restrict $\Gamma_2 = \emptyset$ and $c_0 = 0$. $\forall v_1, v_2 \in V_0$, we have,

$$|a(v_1, v_2)| \leq \|\Delta v_1\|_0 \|\Delta v_2\|_0 + c_1 \|v_1\|_0 \|v_2\|_0 \leq \max\{1, c_1\} \|v_1\|_V \|v_2\|_V.$$

Thus, the bilinear form is continuous. Moreover, it is also coercive, as for any $v \in V_0$,

$$(3.10) \quad \|\nabla v\|_0^2 = - \int_{\Omega} v \Delta v + \int_{\Gamma_0 \cup \Gamma_1 \cup \Gamma_3} v \frac{\partial v}{\partial n} = - \int_{\Omega} v \Delta v \leq \frac{1}{2} \left(\rho \|v\|_0^2 + \frac{1}{\rho} \|\Delta v\|_0^2 \right),$$

where ρ is an arbitrary positive constant. Therefore, $a(v, v) = \|\Delta v\|_0^2 + c_1 \|v\|_0^2 \geq \frac{2}{3} \min\{1, c_1\} \|v\|_V^2$ for $\rho = 1$. Thus, this problem is well-posed by the Lax-Milgram Theorem. \square

Remark 3.4. If $\Gamma_0 \cup \Gamma_1 \neq \emptyset$ in Corollary 3.3, then by the Poincaré inequality, $\|u\|_0^2 \leq c_p \|\nabla u\|_0^2$, where c_p is a positive constant. Any choice of ρ in (3.10) that satisfies $0 < \rho < \frac{2}{c_p}$ implies that Problem (3.2) is well-posed for $c_1 = 0$.

Remark 3.5. When $\partial\Omega = \Gamma_2$ (the analogous case to full Neumann BCs), if $c_0 = 0$, then the problem is not coercive. We illustrate this by considering the harmonic function $v = e^{-kx} \cos(ky)$, for which $a(v, v) = c_1 \|v\|_0^2 = \mathcal{O}(k^{-2})$. On the other hand, $\|v\|_V^2 = \mathcal{O}(k^{-2}) + \mathcal{O}(1)$. Thus, as k gets larger, the implied bound on the coercivity constant goes to zero. Thus, in what follows, c_0 is restricted to be positive if $\Gamma_2 \subseteq \partial\Omega$.

COROLLARY 3.6. Let $\Omega = (0, 1)^d$, $c_0, c_1 \geq 0$, and $\partial\Omega = \Gamma_1$. Assume that the boundary data satisfy the compatibility conditions of [32, Theorem 7.2.2.3]. Then, Problem (3.2) has a unique solution $u \in H^{k+4}(\Omega)$ for $f \in H^k(\Omega)$, where $k \geq 0$.

Proof. This is a direct result of [31, Proposition 1.3] and [32, Theorem 7.2.2.3]. \square

We now turn our attention to the mixed formulation at the continuum level. Letting $\vec{v} = \nabla u$ and $\vec{\alpha} = \nabla \nabla \cdot \vec{v} - c_0 \vec{v}$, (3.1) is equivalent to the following system of first- and second-order PDEs.

$$(3.11) \quad \nabla \cdot \vec{\alpha} + c_1 u = f,$$

$$(3.12) \quad \vec{\alpha} - \nabla \nabla \cdot \vec{v} + c_0 \vec{v} = 0,$$

$$(3.13) \quad \vec{v} - \nabla u = 0.$$

Considering the relevant spaces and applying the boundary conditions given in (3.4)-(3.7), the weak form of (3.11)-(3.13) is to find the triple $(u, \vec{v}, \vec{\alpha}) \in L^2(\Omega) \times H_{g_2}^{\Gamma_1 \cup \Gamma_3}(\text{div}; \Omega) \times H_{g_3}^{\Gamma_2 \cup \Gamma_3}(\text{div}; \Omega)$ such that

$$(3.14) \quad \int_{\Omega} \nabla \cdot \vec{\alpha} \phi + c_1 u \phi = \int_{\Omega} f \phi,$$

$$(3.15) \quad \int_{\Omega} \vec{\alpha} \cdot \vec{\psi} + \nabla \cdot \vec{v} \nabla \cdot \vec{\psi} + c_0 \int_{\Omega} \vec{v} \cdot \vec{\psi} = \int_{\Gamma_0 \cup \Gamma_2} g_1 \vec{\psi} \cdot \vec{n},$$

$$(3.16) \quad \int_{\Omega} \vec{\beta} \cdot \vec{v} + \int_{\Omega} u \nabla \cdot \vec{\beta} = \int_{\Gamma_0 \cup \Gamma_1} g_0 \vec{\beta} \cdot \vec{n},$$

$\forall (\phi, \vec{\psi}, \vec{\beta}) \in L^2(\Omega) \times H_0^{\Gamma_1 \cup \Gamma_3}(\text{div}; \Omega) \times H_0^{\Gamma_2 \cup \Gamma_3}(\text{div}; \Omega)$, where, for $\Gamma \subset \partial\Omega$,

$$H_g^{\Gamma}(\text{div}; \Omega) = \{ \vec{v} \in H(\text{div}; \Omega) \mid \vec{v} \cdot \vec{n} = g \text{ on } \Gamma \}.$$

This weak form is equivalent to the saddle-point problem of finding $(u, \vec{v} - \vec{v}_1, \vec{\alpha} - \vec{\alpha}_1) \in L^2(\Omega) \times H_0^{\Gamma_1 \cup \Gamma_3}(\text{div}; \Omega) \times H_0^{\Gamma_2 \cup \Gamma_3}(\text{div}; \Omega)$ such that

$$(3.17) \quad a((u, \vec{v} - \vec{v}_1), (\phi, \vec{\psi})) + b((\phi, \vec{\psi}), \vec{\alpha} - \vec{\alpha}_1) = F((\phi, \vec{\psi})),$$

$$(3.18) \quad b((u, \vec{v} - \vec{v}_1), \vec{\beta}) = G(\vec{\beta}),$$

$\forall (\phi, \vec{\psi}, \vec{\beta}) \in L^2(\Omega) \times H_0^{\Gamma_1 \cup \Gamma_3}(\text{div}; \Omega) \times H_0^{\Gamma_2 \cup \Gamma_3}(\text{div}; \Omega)$, where $(\vec{v}_1, \vec{\alpha}_1)$ can be any pair in $H_{g_2}^{\Gamma_1 \cup \Gamma_3}(\text{div}; \Omega) \times H_{g_3}^{\Gamma_2 \cup \Gamma_3}(\text{div}; \Omega)$, and the linear and bilinear forms a , b , F , and G are given by

$$(3.19) \quad a((u, \vec{v}), (\phi, \vec{\psi})) = c_0 \int_{\Omega} \vec{v} \cdot \vec{\psi} + \int_{\Omega} \nabla \cdot \vec{v} \nabla \cdot \vec{\psi} + c_1 \int_{\Omega} u \phi,$$

$$(3.20) \quad b((u, \vec{v}), \vec{\beta}) = \int_{\Omega} \vec{\beta} \cdot \vec{v} + u \nabla \cdot \vec{\beta},$$

$$(3.21) \quad F((\phi, \vec{\psi})) = \int_{\Omega} f \phi - \int_{\Omega} (\vec{\alpha}_1 + c_0 \vec{v}_1) \cdot \vec{\psi} - \int_{\Omega} \nabla \cdot \vec{v}_1 \nabla \cdot \vec{\psi} \\ + \int_{\Gamma_0 \cup \Gamma_2} g_1 \vec{\psi} \cdot \vec{n} - \int_{\Omega} \phi \nabla \cdot \vec{\alpha}_1,$$

$$(3.22) \quad G(\vec{\beta}) = - \int_{\Omega} \vec{v}_1 \cdot \vec{\beta} + \int_{\Gamma_0 \cup \Gamma_1} g_0 \vec{\beta} \cdot \vec{n}.$$

As noted above, the boundary conditions imposed can have significant effects on the well-posedness of the problem. In particular, we now show that the mixed-formulation is well-posed under combinations of assumptions on c_0 , c_1 , and the boundary conditions.

THEOREM 3.7. *Assume $\partial\Omega = \Gamma_0 \cup \Gamma_3$. Then the saddle-point problem (3.17)-(3.18) has a unique solution for any $c_0 \geq 0$ and $c_1 > 0$, and for $c_1 \geq 0$ if Γ_0 is nonempty.*

Proof. We verify the standard conditions for well-posedness [18]. Continuity of a , b , F and G in the product norm on $L^2(\Omega) \times H(\operatorname{div}; \Omega) \times H(\operatorname{div}; \Omega)$ is straightforward.

We next show that the bilinear form $a((u, \vec{v}), (\phi, \vec{\psi}))$ is coercive on the set

$$\eta = \{(u, \vec{v}) \in L^2(\Omega) \times H_0^{\Gamma_3}(\operatorname{div}; \Omega) \mid b((u, \vec{v}), \vec{\alpha}) = 0, \quad \forall \vec{\alpha} \in H_0^{\Gamma_3}(\operatorname{div}; \Omega)\}.$$

Since the boundary conditions for \vec{v} and $\vec{\alpha}$ are identical on $\Gamma_0 \cup \Gamma_3$, the kernel condition implies that $b((u, \vec{v}), \vec{v}) = 0$ for any (u, \vec{v}) in η , which implies that $\|\vec{v}\|_0^2 = -\int_{\Omega} u \nabla \cdot \vec{v} \leq \frac{1}{2} (\|u\|_0^2 + \|\nabla \cdot \vec{v}\|_0^2)$. Then

$$\begin{aligned} a((u, \vec{v}), (u, \vec{v})) &= c_0 \|\vec{v}\|_0^2 + \frac{1}{3} (\|\nabla \cdot \vec{v}\|_0^2 + c_1 \|u\|_0^2) + \frac{2}{3} (\|\nabla \cdot \vec{v}\|_0^2 + c_1 \|u\|_0^2) \\ &\geq c_0 \|\vec{v}\|_0^2 + \frac{2 \min\{1, c_1\}}{3} \|\vec{v}\|_0^2 + \frac{2 \min\{1, c_1\}}{3} (\|\nabla \cdot \vec{v}\|_0^2 + \|u\|_0^2) \\ &\geq \frac{2 \min\{1, c_1\}}{3} (\|\vec{v}\|_{\operatorname{div}}^2 + \|u\|_0^2), \end{aligned}$$

where $\|\vec{v}\|_{\operatorname{div}}^2 = \|\vec{v}\|_0^2 + \|\nabla \cdot \vec{v}\|_0^2$.

If Γ_0 is nonempty and $c_1 = 0$, then for a given (u, \vec{v}) , we choose $\vec{\alpha} = \mu \vec{v} + \vec{\alpha}_m$, where μ is a positive constant to be specified below, and $\vec{\alpha}_m$ is the solution of the mixed formulation in Lemma 2.2 with $\Gamma_D = \Gamma_0$, $\Gamma_N = \Gamma_3$, resulting in $\|\vec{\alpha}_m\|_{\operatorname{div}}^2 \leq \Lambda \|u\|_0^2$. Thus, for every $(u, \vec{v}) \in \eta$ and using Remark 2.4, we have

$$b((u, \vec{v}), \vec{\alpha}) = \mu \|\vec{v}\|_0^2 + \|u\|_0^2 + \int_{\Omega} \vec{\alpha}_m \cdot \vec{v} + \mu \int_{\Omega} u \nabla \cdot \vec{v} = 0.$$

Rearranging terms and using the Cauchy-Schwarz and Young's inequalities, we get

$$\frac{\mu}{2} \left(\frac{2\mu}{k_1} \|u\|_0^2 + \frac{k_1}{2\mu} \|\nabla \cdot \vec{v}\|_0^2 \right) + \frac{1}{2} \left(\frac{2}{k_2} \|u\|_0^2 + \frac{k_2 \Lambda}{2} \|\vec{v}\|_0^2 \right) \geq \mu \|\vec{v}\|_0^2 + \|u\|_0^2$$

for arbitrary $k_1 > 0, k_2 > 0$, which can be further rearranged to yield

$$\frac{k_1}{4} \|\nabla \cdot \vec{v}\|_0^2 \geq \left(\mu - \frac{k_2 \Lambda}{4} \right) \|\vec{v}\|_0^2 + \left(1 - \frac{\mu^2}{k_1} - \frac{1}{k_2} \right) \|u\|_0^2.$$

Choosing sufficiently large constants k_1 and μ and sufficiently small k_2 results in the coercivity condition that $a((u, \vec{v}), (u, \vec{v})) = \|\nabla \cdot \vec{v}\|_0^2 \geq K (\|\vec{v}\|_{\operatorname{div}}^2 + \|u\|_0^2)$, for some constant $K > 0$.

Finally, we establish the necessary inf-sup condition, that

$$\sup_{(u, \vec{v}) \in L^2(\Omega) \times H_0^{\Gamma_3}(\operatorname{div}; \Omega)} \frac{b((u, \vec{v}), \vec{\alpha})}{\sqrt{\|u\|_0^2 + \|\vec{v}\|_{\operatorname{div}}^2}} \geq \frac{1}{\sqrt{2}} \|\vec{\alpha}\|_{\operatorname{div}}, \quad \forall \vec{\alpha} \in H_0^{\Gamma_3}(\operatorname{div}; \Omega)$$

The choice $u = \nabla \cdot \vec{\alpha}$, $\vec{v} = \vec{\alpha}$ completes the proof, noting this is compatible with $\partial\Omega = \Gamma_0 \cup \Gamma_3$, since $u \in L^2(\Omega)$, without an essential boundary condition explicitly imposed on it. \square

COROLLARY 3.8. Assume $\partial\Omega = \Gamma_0 \cup \Gamma_2 \cup \Gamma_3$. Then the saddle-point problem (3.17)-(3.18) has a unique solution for any $c_0 > 0$ and $c_1 > 0$.

Proof. Under these assumptions, the bilinear form a is coercive for $(u, \vec{v}) \in L^2(\Omega) \times H_0^{\Gamma_3}(\text{div}; \Omega)$ since

$$(3.23) \quad a((u, \vec{v}), (u, \vec{v})) = c_0 \|\vec{v}\|_0^2 + \|\nabla \cdot \vec{v}\|_0^2 + c_1 \|u\|_0^2 \geq \min\{1, c_0, c_1\} (\|\vec{v}\|_{\text{div}}^2 + \|u\|_0^2).$$

Moreover, the inf-sup condition,

$$\sup_{(u, \vec{v}) \in L^2(\Omega) \times H_0^{\Gamma_3}(\text{div}; \Omega)} \frac{b((u, \vec{v}), \vec{\alpha})}{\sqrt{\|u\|_0^2 + \|\vec{v}\|_{\text{div}}^2}} \geq \frac{1}{\sqrt{2}} \|\vec{\alpha}\|_{\text{div}}, \quad \forall \vec{\alpha} \in H_0^{\Gamma_2 \cup \Gamma_3}(\text{div}; \Omega),$$

is readily shown by choosing $u = \nabla \cdot \vec{\alpha}$, $\vec{v} = \vec{\alpha}$, noting that this is allowable because $\vec{\alpha} \in H_0^{\Gamma_2 \cup \Gamma_3}(\text{div}; \Omega) \subset H_0^{\Gamma_3}(\text{div}; \Omega)$, and $\nabla \cdot \vec{\alpha} \in L^2(\Omega)$. \square

Solving (3.17)–(3.18) when essential boundary conditions on \vec{v} are strongly imposed while $\vec{\alpha}$ is free on the boundary, i.e. $\partial\Omega = \Gamma_1$, leads to difficulties in proving the inf-sup condition. This difficulty can easily be understood from the proof of the inf-sup condition in Theorem 3.7, in which we take $\vec{v} = \vec{\alpha}$ to provide a concrete bound on the supremum. In this setting, we are only able to prove existence of a solution to the continuum mixed form of the problem (under suitable assumptions on the problem data), and not uniqueness.

COROLLARY 3.9. Assume that $f \in H^k(\Omega)$, and $\partial\Omega = \Gamma_1$. Let the boundary data satisfy the compatibility conditions in [32, Theorem 7.2.2.3]. Then the saddle-point problem (3.17)-(3.18) has a solution for any $c_0 \geq 0$ and $c_1 > 0$.

Proof. From Corollary 3.6, the fourth-order form of the problem has solution $u \in H^{k+4}$ under these assumptions. This choice of u solves the mixed formulation with $\vec{v} = \nabla u$ and $\vec{\alpha} = \nabla \nabla \cdot \vec{v} - c_0 \vec{v}$. \square

4. Discrete Analysis. For what follows, we consider a conforming discretization of the mixed form, with

$$(u_h, \vec{v}_h, \vec{\alpha}_h) \in DG_k(\Omega, \tau_h) \times RT_{k+1}^{\Gamma_3}(\Omega, \tau_h) \times RT_{k+1}^{\Gamma_2 \cup \Gamma_3}(\Omega, \tau_h),$$

for $k \geq 0$, where $RT_{k+1}^{\Gamma_3}(\Omega, \tau_h) = \{\vec{v}_h \in RT_{k+1}(\Omega, \tau_h) \mid \vec{v}_h \cdot \vec{n} = 0 \text{ on } \Gamma\}$, noting that $DG_k(\Omega, \tau_h) \subset L^2(\Omega)$ and $RT_{k+1}^{\Gamma_3}(\Omega, \tau_h) \subset H_0^{\Gamma_3}(\text{div}; \Omega)$. Boundary conditions on Γ_1 will be enforced with Nitsche's method. As in the continuum case, taking $\partial\Omega = \Gamma_0 \cup \Gamma_3$ is the easiest case to consider.

COROLLARY 4.1. Let $\partial\Omega = \Gamma_0 \cup \Gamma_3$, $c_0 \geq 0$, $c_1 > 0$, and $c_1 \geq 0$ if Γ_0 is nonempty. Let $\{\tau_h\}$, $0 < h \leq 1$ be a quasiuniform family of triangular meshes of Ω . Then the problem of finding $(u_h, \vec{v}_h - \vec{v}_{1,h}, \vec{\alpha}_h - \vec{\alpha}_{1,h}) \in DG_k(\Omega, \tau_h) \times RT_{k+1}^{\Gamma_3}(\Omega, \tau_h) \times RT_{k+1}^{\Gamma_3}(\Omega, \tau_h)$ such that

$$(4.1) \quad a((u_h, \vec{v}_h - \vec{v}_{1,h}), (\phi_h, \vec{\psi}_h)) + b((\phi_h, \vec{\psi}_h), \vec{\alpha}_h - \vec{\alpha}_{1,h}) = F((\phi_h, \vec{\psi}_h)),$$

$$(4.2) \quad b((u_h, \vec{v}_h - \vec{v}_{1,h}), \vec{\beta}_h) = G(\vec{\beta}_h),$$

$\forall (\phi_h, \vec{\psi}_h, \vec{\beta}_h) \in DG_k(\Omega, \tau_h) \times RT_{k+1}^{\Gamma_3}(\Omega, \tau_h) \times RT_{k+1}^{\Gamma_3}(\Omega, \tau_h)$, has a unique solution for any τ_h in the family. Here, $\vec{v}_{1,h}$, and $\vec{\alpha}_{1,h}$ are taken to be $\Pi_h^{k+1} \vec{v}_1$ and $\Pi_h^{k+1} \vec{\alpha}_1$, where $(\vec{v}_1, \vec{\alpha}_1)$ is the pair employed in (3.17)-(3.18), and Π_h^{k+1} is finite-element interpolation operator defined in Theorem (2.1)

Proof. Coercivity of the bilinear form $a((u_h, \vec{v}_h), (\phi, \vec{\psi}_h))$ on the set

$$\{(u_h, \vec{v}_h) \in DG_k(\Omega, \tau_h) \times RT_{k+1}^{\Gamma_3}(\Omega, \tau_h) \mid b((u_h, \vec{v}_h), \vec{\alpha}_h) = 0, \forall \vec{\alpha} \in RT_{k+1}^{\Gamma_3}(\Omega, \tau_h)\},$$

and the inf-sup condition of the form

$$\sup_{(u_h, \vec{v}_h) \in DG_k(\Omega, \tau_h) \times RT_{k+1}^{\Gamma_3}(\Omega, \tau_h)} \frac{b((u_h, \vec{v}_h), \vec{\alpha}_h)}{\sqrt{\|u_h\|_0^2 + \|\vec{v}_h\|_{\text{div}}^2}} \geq \frac{1}{\sqrt{2}} \|\vec{\alpha}_h\|_{\text{div}}, \quad \forall \vec{\alpha}_h \in RT_{k+1}^{\Gamma_3}(\Omega, \tau_h),$$

can be proven exactly as in the continuum level. Note that this is compatible with the finite-element spaces, i.e. we can choose $\vec{\alpha}_h = \vec{v}_h \in RT_{k+1}^{\Gamma_3}(\tau_h)$ in the kernel condition within the coercivity proof, and $\vec{v}_h = \vec{\alpha}_h \in RT_{k+1}^{\Gamma_3}(\tau_h)$ and $u_h = \nabla \cdot \vec{\alpha}_h$ in the proof of the inf-sup condition. Such a u_h is in $DG_k(\Omega, \tau_h)$ by Remark 2.6. \square

COROLLARY 4.2. *Let the assumptions of Corollary 4.1 hold, and let $u \in H^{k+5}(\Omega)$ be the solution of (3.1). Take $\vec{v} = \nabla u$ and $\vec{\alpha} = \nabla \Delta u - c_0 \nabla u$. Let $(u_h, \vec{v}_h - \vec{v}_{1,h}, \vec{\alpha}_h - \vec{\alpha}_{1,h}) \in DG_k(\Omega, \tau_h) \times RT_{k+1}^{\Gamma_3}(\Omega, \tau_h) \times RT_{k+1}^{\Gamma_3}(\Omega, \tau_h)$ be the solution of (4.1)-(4.2). Then, there exist constants m_1 and m_2 such that*

$$\begin{aligned} \|(u, \vec{v} - \vec{v}_1) - (u_h, \vec{v}_h - \vec{v}_{1,h})\|_{0,\text{div}} &\leq m_1 h^{k+1} \left(|u|_{k+1}^2 + |\vec{v} - \vec{v}_1|_{k+1}^2 + |\nabla \cdot (\vec{v} - \vec{v}_1)|_{k+1}^2 \right. \\ &\quad \left. + |\vec{\alpha} - \vec{\alpha}_1|_{k+1}^2 + |\nabla \cdot (\vec{\alpha} - \vec{\alpha}_1)|_{k+1}^2 \right)^{1/2}, \\ \|(\vec{\alpha} - \vec{\alpha}_1) - (\vec{\alpha}_h - \vec{\alpha}_{1,h})\|_{\text{div}} &\leq m_2 h^{k+1} \left(|u|_{k+1}^2 + |\vec{v} - \vec{v}_1|_{k+1}^2 + |\nabla \cdot (\vec{v} - \vec{v}_1)|_{k+1}^2 \right. \\ &\quad \left. + |\vec{\alpha} - \vec{\alpha}_1|_{k+1}^2 + |\nabla \cdot (\vec{\alpha} - \vec{\alpha}_1)|_{k+1}^2 \right)^{1/2}. \end{aligned}$$

Proof. Because this is a conforming discretization, standard approximation theory for mixed finite elements (e.g. [18]) yields optimal approximation results in the product norm,

$$\|(u_h, \vec{v}_h)\|_{0,\text{div}}^2 = \|u_h\|_0^2 + \|\vec{v}_h\|_{\text{div}}^2. \quad \square$$

Remark 4.3. Corollary 4.2 and the triangle inequality can be used to show that \vec{v}_h and $\vec{\alpha}_h$ are approximations of ∇u and $\nabla \Delta u - c_0 \nabla u$, respectively, with $\mathcal{O}(h^{k+1})$ error estimates.

COROLLARY 4.4. *Consider the weak form (3.17)-(3.18), with $\partial\Omega = \Gamma_0 \cup \Gamma_2 \cup \Gamma_3$. The discretized saddle-point problem*

$$(4.3) \quad a((u_h, \vec{v}_h - \vec{v}_{1,h}), (\phi_h, \vec{\psi}_h)) + b((\phi_h, \vec{\psi}_h), \vec{\alpha}_h - \vec{\alpha}_{1,h}) = F((\phi_h, \vec{\psi}_h)),$$

$$(4.4) \quad b((u_h, \vec{v}_h - \vec{v}_{1,h}), \vec{\beta}_h) = 0,$$

$\forall (\phi_h, \vec{\psi}_h, \vec{\beta}_h) \in DG_k(\Omega, \tau_h) \times RT_{k+1}^{\Gamma_3}(\Omega, \tau_h) \times RT_{k+1}^{\Gamma_2 \cup \Gamma_3}(\Omega, \tau_h)$, has a unique solution $(u_h, \vec{v}_h, \vec{\alpha}_h)$ for $c_0, c_1 > 0$. Here, $\vec{v}_{1,h}$, and $\vec{\alpha}_{1,h}$ are taken to be $\Pi_h^{k+1} \vec{v}_1$ and $\Pi_h^{k+1} \vec{\alpha}_1$, where $(\vec{v}_1, \vec{\alpha}_1)$ is the pair employed in (3.17)-(3.18), and Π_h^{k+1} is finite-element interpolation operator defined in Theorem (2.1).

Proof. The proof is exactly as in the proof of Corollary 3.8. The bilinear form a is coercive for every pair $(u_h, \vec{v}_h) \in DG_k(\Omega, \tau_h) \times RT_{k+1}^{\Gamma_3}(\Omega, \tau_h)$. The finite-element

approximation spaces allow the choice $u_h = \nabla \cdot \vec{\alpha}_h$ and $\vec{v}_h = \vec{\alpha}_h$ for the inf-sup condition. As this is a conforming discretization, standard theory yields optimal approximation results. \square

As in the continuum case, solving (4.1)–(4.2) when essential boundary conditions on \vec{v} are strongly imposed while $\vec{\alpha}$ is free on the boundary leads to difficulties in proving the inf-sup condition. When $\partial\Omega = \Gamma_1$, we cannot follow the proof technique used in Theorem 3.7 and Corollary 3.8, since \vec{v} must satisfy the prescribed BC while $\vec{\alpha}$ is free on the boundary. In this case, the inf-sup condition has the form of finding $\tilde{c} > 0$ such that

$$\begin{aligned} I &= \sup_{(u_h, \vec{v}_h) \in DG_k(\Omega, \tau_h) \times RT_{k+1}^{\Gamma_1}(\Omega, \tau_h)} \frac{\int_{\Omega} \vec{\alpha}_h \cdot \vec{v}_h + \int_{\Omega} u_h \nabla \cdot \vec{\alpha}_h}{\sqrt{\|u_h\|_0^2 + \|\vec{v}_h\|_{\text{div}}^2}} \\ &> \tilde{c} \|\vec{\alpha}_h\|_{\text{div}}, \quad \forall \vec{\alpha}_h \in RT_{k+1}(\Omega, \tau_h). \end{aligned}$$

To understand the challenge, we consider the two-dimensional discrete Helmholtz decomposition from Lemma 2.5,

$$RT_{k+1}(\Omega, \tau_h) = \left(\nabla \times CG_{k+1}(\Omega, \tau_h) \right) \oplus \left(\text{grad}_h DG_k(\Omega, \tau_h) \right).$$

For any $\vec{\alpha}_h = \text{grad}_h z$ where $z \in DG_k(\Omega, \tau_h)$, then the choice $\vec{v}_h = 0$ and $u_h = \nabla \cdot \vec{\alpha}_h - z$ satisfies the inf-sup condition, as

$$\begin{aligned} I &\geq \sup_{u_h \neq 0 \in DG_k(\Omega, \tau_h)} \frac{\int_{\Omega} u_h \nabla \cdot \vec{\alpha}_h}{\|u_h\|_0} \geq \frac{\|\nabla \cdot \vec{\alpha}_h\|_0^2 - \int_{\Omega} z \nabla \cdot (\text{grad}_h z)}{\|\nabla \cdot \vec{\alpha}_h\|_0 + \|z\|_0} \\ &\geq \frac{\|\nabla \cdot \vec{\alpha}_h\|_0^2 + \|\text{grad}_h z\|_0^2}{\|\nabla \cdot \vec{\alpha}_h\|_0 + c \|\text{grad}_h z\|_0} \geq \tilde{c} (\|\nabla \cdot \vec{\alpha}_h\|_0 + \|\vec{\alpha}_h\|_0), \end{aligned}$$

where the discrete Poincaré inequality [6], $\|z\|_0 \leq c \|\text{grad}_h z\|_0$, is used here. In contrast, for $\vec{\alpha}_h \in \nabla \times CG_{k+1}(\Omega, \tau_h)$, we cannot establish a uniform inf-sup condition. As a simple example, take $\Omega = (0, 1)^2$, with $\partial\Omega = \Gamma_1$, and consider $k = 0$, so $\vec{\alpha}_h \in RT_1(\Omega, \tau_h)$. Consider a mesh such that one triangle has vertices $(0, 0)$, $(h, 0)$, and $(0, h)$. Take $\vec{\alpha}_h$ to be nonzero only in this triangle, with value

$$(4.5) \quad \vec{\alpha}_h = \nabla \times \left(1 - \frac{x+y}{h} \right) = \frac{1}{h} \begin{bmatrix} -1 \\ 1 \end{bmatrix}.$$

Clearly, $\nabla \cdot \vec{\alpha}_h = 0$. Moreover, for any choice of $\vec{v}_h \in RT_1(\Omega, \tau_h)$ with $\vec{v}_h \cdot \vec{n} = 0$ on $\partial\Omega$ and $u_h \in DG_0(\tau_h)$, we have $\int_{\Omega} \vec{\alpha}_h \cdot \vec{v}_h + \int_{\Omega} u_h \nabla \cdot \vec{\alpha}_h = 0$, which results in a zero inf-sup constant. Restricting the mesh so that no element has 3 vertices on the boundary appears to lead to an $\mathcal{O}(h)$ inf-sup constant.

We next show that weakly implementing the essential boundary condition on \vec{v} yields a discretization with $\mathcal{O}(h^{-1/2})$ continuity constant and $\mathcal{O}(h^{1/2})$ inf-sup constant, but without any mesh restrictions. This is advantageous because the error estimate is linear in the continuity constant but quadratic in the inf-sup constant, and the overall quasi-optimality constant is superior to the $\mathcal{O}(1)$ continuity constant but $\mathcal{O}(h)$ inf-sup constant observed (but not proven) above. We will make use of a Nitsche-type penalty method. These approaches are based on adding three terms to the weak form, which are commonly denoted as the consistency, stability, and symmetry terms [33, 48]. There is a natural tension between achieving symmetry in the

resulting bilinear form and proving coercivity; we choose to make a non-symmetric modification to the bilinear form, for which coercivity is easily proven. Consider the case where $\partial\Omega = \Gamma_0 \cup \Gamma_1 \cup \Gamma_3$, and modify the bilinear form $a((u, \vec{v}), (\phi, \vec{\psi}))$ and linear form $F((\phi, \vec{\psi}))$ from (3.19) and (3.21), to be

$$(4.6) \quad \hat{a}((u_h, \vec{v}_h - \vec{v}_{1,h}), (\phi_h, \vec{\psi}_h)) + b((\phi_h, \vec{\psi}_h), \vec{\alpha}_h - \vec{\alpha}_{1,h}) = \hat{F}((\phi_h, \vec{\psi}_h)),$$

$$(4.7) \quad b((u_h, \vec{v}_h - \vec{v}_{1,h}), \vec{\beta}_h) = G(\vec{\beta}_h),$$

$\forall (\phi_h, \vec{\psi}_h, \vec{\beta}_h) \in DG_k(\Omega, \tau_h) \times RT_{k+1}^{\Gamma_3}(\Omega, \tau_h) \times RT_{k+1}^{\Gamma_3}(\Omega, \tau_h)$, where,

$$(4.8) \quad \begin{aligned} \hat{a}((u, \vec{v}), (\phi, \vec{\psi})) &= c_0 \int_{\Omega} \vec{v} \cdot \vec{\psi} + \int_{\Omega} \nabla \cdot \vec{v} \nabla \cdot \vec{\psi} + c_1 \int_{\Omega} u \phi - \int_{\Gamma_1} \nabla \cdot \vec{v} \vec{\psi} \cdot \vec{n} \\ &+ \int_{\Gamma_1} \nabla \cdot \vec{\psi} \vec{v} \cdot \vec{n} + \lambda \int_{\Gamma_1} \vec{v} \cdot \vec{n} \vec{\psi} \cdot \vec{n}, \\ \hat{F}((\phi, \vec{\psi})) &= \int_{\Omega} f \phi - \int_{\Omega} (\vec{\alpha}_{1,h} + c_0 \vec{v}_{1,h}) \cdot \vec{\psi} - \int_{\Omega} \nabla \cdot \vec{v}_{1,h} \nabla \cdot \vec{\psi} \\ &+ \int_{\Gamma_0} g_1 \vec{\psi} \cdot \vec{n} - \int_{\Omega} \phi \nabla \cdot \vec{\alpha}_{1,h} \\ &+ \int_{\Gamma_1} \nabla \cdot \vec{\psi} g_2 + \lambda \int_{\Gamma_1} \vec{\psi} \cdot \vec{n} g_2 + \int_{\Gamma_1} \nabla \cdot \vec{v}_{1,h} \vec{\psi} \cdot \vec{n} - \int_{\Gamma_1} \nabla \cdot \vec{\psi} \vec{v}_{1,h} \cdot \vec{n} \\ (4.9) \quad &- \lambda \int_{\Gamma_1} \vec{v}_{1,h} \cdot \vec{n} \vec{\psi} \cdot \vec{n}. \end{aligned}$$

Here, we impose the condition that $(\vec{v}_h + \vec{v}_{1,h}) \cdot \vec{n} = g_2$ on Γ_1 directly by adding $\lambda \int_{\Gamma_1} \vec{v} \cdot \vec{n} \vec{\psi} \cdot \vec{n}$ to a as defined in (3.19) and $\lambda \int_{\Gamma_1} (g_2 - \vec{v}_{1,h} \cdot \vec{n}) \vec{\psi} \cdot \vec{n}$ to the linear form, $F(\cdot)$, defined in (3.21), for penalty parameter $\lambda > 0$. In order to prove coercivity, we similarly add terms $\int_{\Gamma_1} \nabla \cdot \vec{\psi} ((\vec{v} + \vec{v}_{1,h}) \cdot \vec{n} - g_2)$ to both sides as appropriate. Finally, for consistency, we include $\int_{\Gamma_1} \nabla \cdot (\vec{v} + \vec{v}_{1,h}) \vec{\psi} \cdot \vec{n}$ on both sides with opposite sign. With these Nitsche terms, we now prove well-posedness of the weak form, but using a modified norm for \vec{v} , defined as

$$\|\vec{v}\|_{\text{div}, \Gamma_1}^2 = \|\vec{v}\|_{\text{div}}^2 + \|\vec{v} \cdot \vec{n}\|_{0, \Gamma_1}^2.$$

THEOREM 4.5. *Let $\Omega \subset \mathbb{R}^d$, $d \in \{2, 3\}$, with $\partial\Omega = \Gamma_0 \cup \Gamma_1 \cup \Gamma_3$. Let $\{\tau_h\}$, $0 < h \leq 1$, be a quasiuniform family of meshes of Ω , and let $\lambda > 0$ be given. The weak form in (4.6)–(4.7) has a unique solution for $c_0 \geq 0$, $c_1 > 0$, and for $c_1 = 0$ if $\Gamma_0 \cup \Gamma_1$ is nonempty.*

Proof. As above, the existence and uniqueness of solutions follows from standard theory. We first show that the bilinear form $\hat{a}((u_h, \vec{v}_h), (\phi_h, \vec{\psi}_h))$ is coercive for any pair $(u_h, \vec{v}_h) \in \eta_h$, where

$$\begin{aligned} \eta_h &= \{(u_h, \vec{v}_h) \in DG_k(\Omega, \tau_h) \times RT_{k+1}^{\Gamma_3}(\Omega, \tau_h) \mid \\ &b((u_h, \vec{v}_h), \vec{\alpha}_h) = 0, \quad \forall \vec{\alpha}_h \in RT_{k+1}^{\Gamma_3}(\Omega, \tau_h)\}. \end{aligned}$$

Since the strongly imposed boundary conditions for \vec{v} and $\vec{\alpha}$ are identical, the kernel condition implies that $b((u_h, \vec{v}_h), \vec{v}_h) = 0$. Thus, any pair $(u_h, \vec{v}_h) \in \eta_h$ should satisfy $\|\vec{v}_h\|_0^2 = -\int_{\Omega} u_h \nabla \cdot \vec{v}_h \leq \frac{1}{2} (\|u_h\|_0^2 + \|\vec{v}_h\|_0^2)$. Employing the Cauchy-Schwarz

inequality, we then have

$$\begin{aligned}
\hat{a}((u_h, \vec{v}_h), (u_h, \vec{v}_h)) &= c_0 \|\vec{v}_h\|_0^2 + \|\nabla \cdot \vec{v}_h\|_0^2 + c_1 \|u_h\|_0^2 + \lambda \|\vec{v}_h \cdot \vec{n}\|_{0, \Gamma_1}^2 \\
&\geq c_0 \|\vec{v}_h\|_0^2 + \frac{\min\{1, c_1\}}{3} (\|\nabla \cdot \vec{v}_h\|_0^2 + \|u_h\|_0^2) \\
&\quad + \frac{2 \min\{1, c_1\}}{3} (\|\nabla \cdot \vec{v}_h\|_0^2 + \|u_h\|_0^2) + \lambda \|\vec{v}_h \cdot \vec{n}\|_{0, \Gamma_1}^2 \\
&\geq \left(c_0 + \frac{2 \min\{1, c_1\}}{3} \right) \|\vec{v}_h\|_0^2 \\
&\quad + \frac{2 \min\{1, c_1\}}{3} (\|\nabla \cdot \vec{v}_h\|_0^2 + \|u_h\|_0^2) + \lambda \|\vec{v}_h \cdot \vec{n}\|_{0, \Gamma_1}^2.
\end{aligned}$$

Clearly, any choice of $\lambda > 0$ completes the proof. Taking, for example, $\lambda = \frac{2}{3}$ gives a coercivity constant of $\frac{2 \min\{1, c_1\}}{3}$. When $\Gamma_0 \cup \Gamma_1$ is nonempty and $c_0 = 0$, the coercivity proof is similar to the one in Theorem 3.7 with $\Gamma_D = \Gamma_0 \cup \Gamma_1$.

Continuity of \hat{a} , b , \hat{F} , and G , can be established using techniques similar to the above and the results of Corollary 2.9 and Remark 2.11, making use of $\|\cdot\|_{\text{div}, \Gamma_1}$ for $\vec{v}_h \in RT_{k+1}^{\Gamma_3}(\Omega, \tau_h)$, and the standard L^2 and $H(\text{div})$ norms for u_h and α_h . The resulting inequalities are that

$$\begin{aligned}
\hat{a}((u_h, \vec{v}_h), (\phi_h, \vec{\psi}_h)) &\leq c_0 \|\vec{v}_h\|_0 \|\vec{\psi}_h\|_0 + \|\nabla \cdot \vec{v}_h\|_0 \|\nabla \cdot \vec{\psi}_h\|_0 + c_1 \|u_h\|_0 \|\phi_h\|_0 \\
&\quad + \|\nabla \cdot \vec{v}_h\|_{0, \Gamma_1} \|\vec{\psi}_h \cdot \vec{n}\|_{0, \Gamma_1} + \|\nabla \cdot \vec{\psi}_h\|_{0, \Gamma_1} \|\vec{v}_h \cdot \vec{n}\|_{0, \Gamma_1} \\
&\quad + \lambda \|\vec{v}_h \cdot \vec{n}\|_{0, \Gamma_1} \|\vec{\psi}_h \cdot \vec{n}\|_{0, \Gamma_1} \\
&\leq (1 + c_0 + c_1 + \lambda) \|(u_h, \vec{v}_h)\|_{0, \text{div}, \Gamma_1} \left\| (\phi_h, \vec{\psi}_h) \right\|_{0, \text{div}, \Gamma_1} \\
&\quad + \frac{\mu}{\sqrt{h}} \left(\|\nabla \cdot \vec{v}_h\|_0 \|\vec{\psi}_h \cdot \vec{n}\|_{0, \Gamma_1} + \|\nabla \cdot \vec{\psi}_h\|_0 \|\vec{v}_h \cdot \vec{n}\|_{0, \Gamma_1} \right) \\
&\leq \left(1 + c_0 + c_1 + \frac{2\mu}{\sqrt{h}} + \lambda \right) \|(u_h, \vec{v}_h)\|_{0, \text{div}, \Gamma_1} \left\| (\phi_h, \vec{\psi}_h) \right\|_{0, \text{div}, \Gamma_1} \blacksquare
\end{aligned}$$

and

$$b((u_h, \vec{v}_h), \vec{\alpha}_h) \leq \|(u_h, \vec{v}_h)\|_{0, \text{div}, \Gamma_1} \|\vec{\alpha}_h\|_{\text{div}},$$

where $\mu = \sqrt{C_\Omega(k+1)(k+d)}$, and $\|(u_h, \vec{v}_h)\|_{0, \text{div}, \Gamma_1}^2 = \|u_h\|_0^2 + \|\vec{v}_h\|_{\text{div}, \Gamma_1}^2$. Thus, the continuity constant of the bilinear form \hat{a} is $\mathcal{O}(h^{-\frac{1}{2}})$.

Finally, we consider the inf-sup condition, that $\exists \gamma > 0$ such that

$$I = \sup_{(u_h, \vec{v}_h) \in DG_k(\Omega, \tau_h) \times RT_{k+1}^{\Gamma_3}(\Omega, \tau_h)} \frac{\int_\Omega \vec{\alpha}_h \cdot \vec{v}_h + \int_\Omega u_h \nabla \cdot \vec{\alpha}_h}{\sqrt{\|\vec{v}_h\|_{\text{div}, \Gamma_1}^2 + \|u_h\|_0^2}} \geq \gamma \|\vec{\alpha}_h\|_{\text{div}}, \quad \forall \vec{\alpha}_h \in RT_{k+1}^{\Gamma_3}(\Omega, \tau_h). \blacksquare$$

The choice $\vec{v}_h = \vec{\alpha}_h$ and $u_h = \nabla \cdot \vec{\alpha}_h$ and the inverse trace inequality from Corollary

2.9 and Remark 2.11 imply that

$$\begin{aligned}
I &\geq \frac{\|\vec{\alpha}_h\|_{\text{div}}^2}{\sqrt{\|\vec{\alpha}_h\|_{\text{div}}^2 + \|\vec{\alpha}_h \cdot \vec{n}\|_{0,\Gamma_1}^2 + \|\nabla \cdot \vec{\alpha}_h\|_0^2}} \\
&\geq \frac{\|\vec{\alpha}_h\|_{\text{div}}^2}{\sqrt{\|\vec{\alpha}_h\|_{\text{div}}^2 + \frac{C_\Omega(k+2)(k+d+1)}{h} \|\vec{\alpha}_h\|_0^2 + \|\nabla \cdot \vec{\alpha}_h\|_0^2}} \\
&\geq \frac{\sqrt{h}}{\sqrt{C_\Omega(k+2)(k+d+1)}} \|\vec{\alpha}_h\|_{\text{div}}. \quad \square
\end{aligned}$$

While the above result establishes the existence and uniqueness of discrete solutions, we note that the inf-sup constant is $\mathcal{O}(h^{\frac{1}{2}})$ and the continuity constant is $\mathcal{O}(h^{-\frac{1}{2}})$, owing to the contribution from the boundary terms in the formulation. The following results apply standard theory (see, e.g., [18]) to provide error estimates for the resulting discrete solutions. For given functions u , \vec{v} , and $\vec{\alpha}$, we define the standard approximation properties of the discrete spaces as

$$\begin{aligned}
E_{(u,\vec{v})} &= \inf_{(\phi_h, \vec{\psi}_h) \in DG_k(\Omega, \tau_h) \times RT_{k+1}^{\Gamma_3}(\Omega, \tau_h)} \|(u, \vec{v}) - (\phi_h, \vec{\psi}_h)\|_{0,\text{div},\Gamma_1}, \\
E_{\vec{\alpha}} &= \inf_{\vec{\beta}_h \in RT_{k+1}^{\Gamma_3}(\Omega, \tau_h)} \|\vec{\alpha} - \vec{\beta}_h\|_{\text{div}},
\end{aligned}$$

where, as above, we use the product norm $\|(u_h, \vec{v}_h)\|_{0,\text{div},\Gamma_1}^2 = \|u_h\|_0^2 + \|\vec{v}_h\|_{\text{div},\Gamma_1}^2$.

COROLLARY 4.6. *Let the assumptions of Theorem 4.5 be satisfied, $\lambda > 0$, and let u be the solution of (3.1) with boundary conditions in (3.4) and (3.5). Take $\vec{v} = \nabla u$ and $\vec{\alpha} = \nabla \Delta u - c_0 \nabla u$. Let $(u_h, \vec{v}_h - \vec{v}_{1,h}, \vec{\alpha}_h - \vec{\alpha}_{1,h})$ be the unique solution of Problem (4.6)-(4.7). Then,*

$$\begin{aligned}
\|(u, \vec{v} - \vec{v}_1) - (u_h, \vec{v}_h - \vec{v}_{1,h})\|_{0,\text{div}} &\leq \left(\frac{4\|\hat{a}\|\|b\|}{h\zeta\gamma} \right) E_{(u,\vec{v}-\vec{v}_1)} + \frac{\|b\|}{\zeta} E_{(\vec{\alpha}-\vec{\alpha}_1)}, \\
\|(\vec{\alpha} - \vec{\alpha}_1) - (\vec{\alpha}_h - \vec{\alpha}_{1,h})\|_{\text{div}} &\leq \left(\frac{2\|\hat{a}\|^2}{\zeta\gamma h^{\frac{3}{2}}} + \frac{3\|\hat{a}\|\|b\|}{\gamma^2 h^{\frac{3}{2}}} \right) E_{(u,\vec{v}-\vec{v}_1)} + \frac{3\|\hat{a}\|\|b\|}{\zeta\gamma h} E_{(\vec{\alpha}-\vec{\alpha}_1)},
\end{aligned}$$

where the constants

$$\begin{aligned}
\|\hat{a}\| &= 1 + c_0 + c_1 + 2\sqrt{C_\Omega(k+1)(k+d)} + \lambda, \\
\|b\| &= 1, \\
\zeta &= \frac{2\min\{1, c_1\}}{3}, \\
\gamma &= \frac{1}{\sqrt{C_\Omega(k+2)(k+d+1)}},
\end{aligned}$$

are the continuity, coercivity, and inf-sup constants from Theorem 4.5, with constants arranged to explicitly show the dependence on h .

Remark 4.7. Corollary 4.6 and the triangle inequality can be used to show that \vec{v}_h and $\vec{\alpha}_h$ are the approximations of ∇u and $\nabla \Delta u - c_0 \nabla u$, respectively with the same error estimates.

5. Monolithic multigrid. We now consider the development of effective linear solvers for the resulting discretized systems. We first consider the case where $\partial\Omega = \Gamma_0 \cup \Gamma_2 \cup \Gamma_3$ with constants $c_0, c_1 > 0$; however, the same arguments allow the case where $c_0 = 0$ if Γ_2 is empty. The discretizations above lead to block-structured linear systems that can be written as

$$(5.1) \quad \begin{bmatrix} A_{11} & 0 & B_1^T \\ 0 & A_{22} & B_2^T \\ B_1 & B_2 & 0 \end{bmatrix} \begin{bmatrix} u \\ \vec{v} \\ \vec{\alpha} \end{bmatrix} = \begin{bmatrix} f_1 \\ f_2 \\ g \end{bmatrix},$$

where $[u, \vec{v}, \vec{\alpha}]^T$ now refers to the vector of coefficients of the finite element basis functions. For the weak form in (3.17)-(3.18), A_{11} is a mass matrix representing the discrete version of the $L^2(\Omega)$ inner product on $DG_k(\Omega, \tau_h)$ weighted by c_1 , A_{22} is the discrete version of the $H(\text{div}; \Omega)$ inner product on $RT_{k+1}(\Omega, \tau_h)$ with weight c_0 on the $L^2(\Omega)$ term, B_1 is the weak gradient operator, and B_2 is the $L^2(\Omega)$ inner product on $RT_{k+1}(\Omega, \tau_h)$.

In order to efficiently solve such linear systems, we consider preconditioned Krylov subspace methods. Two families of preconditioners are popular for such block-structured problems. Block factorization methods [25, 29] approximate Gaussian elimination applied to the blocks of the discretization matrix, writing

$$A = \begin{bmatrix} A & B^T \\ B & -C \end{bmatrix} = \begin{bmatrix} I & 0 \\ BA^{-1} & I \end{bmatrix} \begin{bmatrix} A & 0 \\ 0 & S \end{bmatrix} \begin{bmatrix} I & A^{-1}B^T \\ 0 & I \end{bmatrix},$$

where $S = -(C + BA^{-1}B^T)$ is the Schur complement of A , assuming A is invertible. Natural block preconditioners are of block diagonal, \mathbf{P}_d , and block triangular, \mathbf{P}_t form, given as

$$\mathbf{P}_d = \begin{bmatrix} A & 0 \\ 0 & \hat{S} \end{bmatrix}, \quad \mathbf{P}_t = \begin{bmatrix} A & B^T \\ 0 & -\hat{S} \end{bmatrix},$$

where \hat{S} is some approximation of S . The quality of these preconditioners naturally depends on the approximation $\hat{S} \approx S$, and their efficiency depends on the availability of effective fast solvers for the linear systems involving A and \hat{S} . Preliminary experiments in this direction revealed some difficulties caused by the Nitsche terms that would require further investigation. Therefore, we focus on the development of efficient monolithic multigrid preconditioners [3, 45] in this setting.

We use standard multigrid V -cycles with a direct solve at the coarsest level (taken in the examples to be the mesh with $h = 1/4$ for problems on unit-length domains), and factor-2 coarsening between all grids. These cycles are employed as preconditioners for FGMRES [52]. We use standard interpolation operators, partitioned based on the discretized fields, of the form

$$P = \begin{bmatrix} P_1^k & & \\ & P_2^{k+1} & \\ & & P_2^{k+1} \end{bmatrix},$$

where the blocks P_1^k and P_2^{k+1} are the natural finite-element interpolation operators for the $DG_k(\Omega, \tau_h)$ and $RT_{k+1}(\Omega, \tau_h)$ spaces, respectively. Coarse-grid operators are formed by rediscrretization, which is equivalent to a Galerkin coarse-grid operator for constant $c_0, c_1 \in \mathbb{R}$.

The main challenge with monolithic multigrid methods is to develop an effective relaxation method. In this work, as relaxation we make use of an additive overlapping Schwarz relaxation, which can be considered as a variant of the family of Vanka relaxation schemes originally proposed in [53] to solve the saddle-point systems that arise from the marker-and-cell (MAC) finite-difference discretization of the Navier-Stokes equations. Vanka relaxation methods encompass a variety of overlapping multiplicative or additive Schwarz methods applied to saddle-point problems, in which the subdomains are chosen so that the corresponding subsystems are also saddle-point systems. Vanka-type relaxation has been used extensively for finite-element discretizations, such as the discretizations arising from the Stokes equations [41], magnetohydrodynamics [2], and liquid crystals [1]. Recently, a general-purpose implementation of patch-based relaxation schemes, including Vanka relaxation, was provided in [28], which we employ via the finite-element discretization package Firedrake [39, 50].

Like other Schwarz methods, Vanka relaxation can be understood algebraically. Denoting the set of all degrees of freedom in the problem by Q , we partition Q into s overlapping subdomains or patches, $Q = \cup_{i=1}^s Q_i$, and consider the stationary additive iteration with updates given by

$$x \leftarrow x + \sum_{i=1}^s R_i^T \mathcal{A}_{ii}^{-1} R_i (b - \mathcal{A}x),$$

where $\mathcal{A}x = b$ represents the linear system to be solved, R_i is the injection operator from a global vector, x , to a local vector, x_i , on Q_i (with $R_i x = x_i$), and $\mathcal{A}_{ii} = R_i \mathcal{A} R_i^T$ is the restriction of the global system \mathcal{A} to the degrees of freedom in Q_i . While inexact solution of the subdomain problems is relevant when the cardinality of Q_i is large, we consider small subdomain sizes, where direct solution remains practical. We construct the patches, $\{Q_i\}$, topologically, as the so-called star patch around each vertex [28] in the mesh, taking all degrees of freedom on vertex i , on edges adjacent to vertex i , and on all cells adjacent to vertex i to form Q_i . Figure 1 shows the subdomain construction around a typical vertex for the cases of discretization using DG_0 and RT_1 elements (left) and using DG_1 and RT_2 elements (right), noting that the RT_k degrees of freedom for both \vec{v} and $\vec{\alpha}$ are included in the patch (and are collocated on the mesh). Rather than use the stationary iteration given above, we use two steps of GMRES preconditioned by the Schwarz method as the (pre- and post-)relaxation in the multigrid cycle on each level.

For the case where $\partial\Omega = \Gamma_0 \cup \Gamma_1$ with $c_0 = c_1 = 0$, a modification of the above solver framework is needed. Note that, in this case, while the linear system is well-posed by Theorem 4.5, the modified weak form in (4.6)-(4.7) has the same structure as (5.1) except that A_{11} becomes the zero matrix and Nitsche boundary terms appear in A_{22} . The approach above performs poorly in this case, as might be expected, particularly with the zero block for A_{11} . To overcome this, we adopt the idea of preconditioning the resulting discretization matrix using an auxiliary operator that corresponds to the discretization of another PDE, related to the inner products in which the PDE is analyzed [37, 43]. Here, since the biharmonic operator is equivalent to the norm in Lemma 3.1, we add a scaling factor times the $L^2(\Omega)$ inner product in the (1,1) block of the auxiliary operator. Preliminary experiments (reported below in Table 4) indicate that choosing the scaling factor to be $\mathcal{O}(\frac{1}{h})$ gives better performance than $\mathcal{O}(1)$ values.

6. Numerical experiments. In this section, we present numerical experiments to measure finite-element convergence rates and demonstrate the performance of the

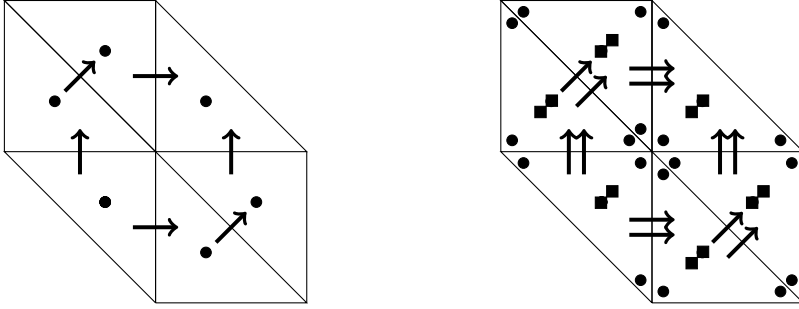


Fig. 1: Star patches for $DG_0 - RT_1$ (left) and $DG_1 - RT_2$ (right) discretizations. Filled discs denote DG degrees of freedom, while arrows and filled squares denote edge and interior RT degrees of freedom, respectively.

proposed monolithic multigrid method, stopping when either the residual norm or its relative reduction is less than 10^{-8} . These numerical results were calculated using the finite-element discretization package Firedrake [50], which offers close integration with PETSc for the linear solvers [12, 39]. The relaxation scheme is implemented using the PCPATCH framework [28]. All numerical experiments were run on a workstation with dual 8-core Intel Xeon 1.7 GHz CPUs and 384 GB of RAM. For reproducibility, the codes used to generate the numerical results, as well as the major Firedrake components needed, have been archived on Zenodo [57].

To measure solution quality, we make use of the method of manufactured solutions, prescribing forcing terms and boundary data to exactly match those of a known solution, u_{ex} . Taking uniform meshes, as described below, with representative mesh size h , we define u_h to be the finite-element solution on the mesh, and define the approximation error $e_h = u_{ex} - u_h$. With this, we can define the relative error in the $L^2(\Omega)$ norm on mesh h as $R_e(h)$, given by

$$R_e(u, h) = \frac{\left(\int_{\Omega} e_h^2 dx \right)^{\frac{1}{2}}}{\left(\int_{\Omega} u_{ex}^2 dx \right)^{\frac{1}{2}}},$$

As needed, we extend these definitions to other quantities, such as the $L^2(\Omega)$ error in \vec{v} and $\vec{\alpha}$, the error in \vec{v} and $\vec{\alpha}$ in the $H(\text{div})$ (semi-)norm, and the error in any boundary terms included in the norms used above.

6.1. 2D Experiments. In 2D, we consider experiments on the unit square using uniform “right” triangular meshes (Figure 2, left) and on the L-shaped domain with vertices $(0, 0)$, $(0, 1)$, $(\frac{1}{2}, 1)$, $(\frac{1}{2}, \frac{1}{2})$, $(1, \frac{1}{2})$, and $(1, 0)$ using uniform “crossed” triangular meshes (Figure 2, right). In both cases, we consider the smooth exact solution $u_{1ex} = \sin(2\pi x) \cos(3\pi y)$ and an exact solution that is in $H^4(\Omega)$, but not $H^p(\Omega)$ for any integer $p > 4$, given by $u_{2ex} = \left(\sin(2\pi x) + x^{\frac{9}{2}} \right) \left(\cos(3\pi y) + y^{\frac{17}{4}} \right)$. The discretizations proposed here have larger numbers of degrees of freedom and nonzeros in their matrices than are typically encountered with Lagrange elements for second-order problems. We therefore record the matrix dimensions, N , and number of nonzeros, nnz , in Table 1 for the discretizations on the unit square, for several levels

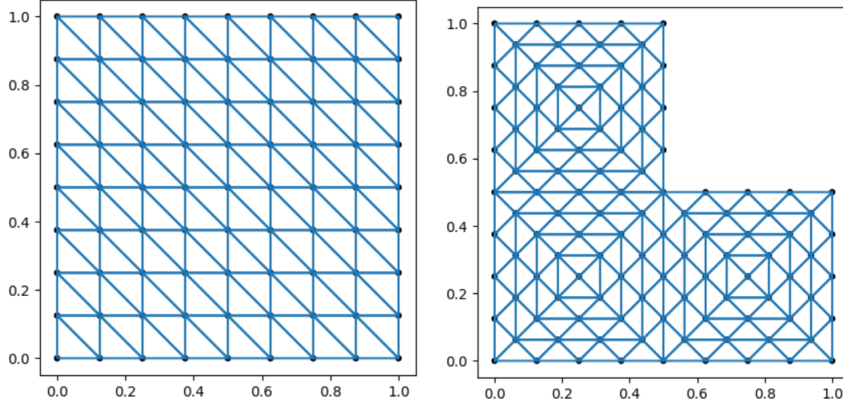


Fig. 2: Left: unit square domain with uniform right triangular mesh ($h = \frac{1}{8}$). Right: L-shaped domain with uniform crossed triangular mesh ($h = \frac{1}{8}$).

Table 1: Dimension N and the number of nonzeros nnz in the system matrix for $u \in DG_k(\Omega, \tau_h)$, $\vec{v} \in RT_{k+1}(\Omega, \tau_h)$, $\vec{\alpha} \in RT_{k+1}(\Omega, \tau_h)$ on uniform meshes of the unit square domain in 2D.

	$k = 0$		$k = 1$		$k = 2$	
$1/h$	N	nnz	N	nnz	N	nnz
2^6	33,024	352,768	107,008	2,762,752	221,952	10,179,072
2^7	131,584	1,410,048	427,008	11,046,912	886,272	40,707,072
2^8	525,312	5,638,144	1,705,984	44,179,456	3,542,016	162,809,856
2^9	2,099,200	22,548,480	6,819,840	176,701,440	14,161,920	651,202,560

of refinement, h , and orders of the discretization, k . In all figures, we use blue, red, and green lines to present results for $k = 0, 1, 2$, respectively, with filled discs denoting the measured (u, v) error in the $L^2 \times H(\text{div})$ norm, and squares denoting the error in α measured in the $H(\text{div})$ norm.

In the first two examples, we consider the unit square domain and plot $\log(R_e(\cdot, h))$ against $\log_2(1/h)$, so that the slopes of the lines represent the experimentally measured convergence rates for $(u, \vec{v}, \vec{\alpha}) \in DG_k(\Omega, \tau_h) \times RT_{k+1}(\Omega, \tau_h) \times RT_{k+1}(\Omega, \tau_h)$, for $k = \{0, 1, 2\}$. Let $\partial\Omega = \Gamma_N \cup \Gamma_S \cup \Gamma_E \cup \Gamma_W$, meaning the North, South, East, and West faces of the square. Figure 3 presents results for the problem with $c_0 = 0$ and $c_1 = 1$ with boundary $\partial\Omega = \Gamma_0 \cup \Gamma_3$, where $\Gamma_0 = \Gamma_E \cup \Gamma_W$, and $\Gamma_3 = \Gamma_N \cup \Gamma_S$. Figure 4 presents results when $c_0 = 2$, $c_1 = 4$, and $\partial\Omega = \Gamma_0 \cup \Gamma_2 \cup \Gamma_3$ with $\Gamma_0 = \Gamma_E \cup \Gamma_W$, $\Gamma_2 = \Gamma_S$, and $\Gamma_3 = \Gamma_N$. Since we omit Γ_1 from these examples, there is no need to use the Nitsche boundary terms considered in that case. We note that we see optimal convergence for all k with (u, \vec{v}) in the $L^2 \times H(\text{div})$ norm and $\vec{\alpha}$ in the $H(\text{div})$ norm for the smooth exact solution, u_{1ex} , on the left of these figures. Considering the $H^4(\Omega)$ solution, u_{2ex} , on the right, we see optimal convergence for small k , but degraded performance for $k = 2$, where the lack of smoothness in α is reflected in the numerical results. These results are consistent with the analysis in Corollaries 4.2 and 4.4, although we note that the $H^4(\Omega)$ case outperforms the expected convergence

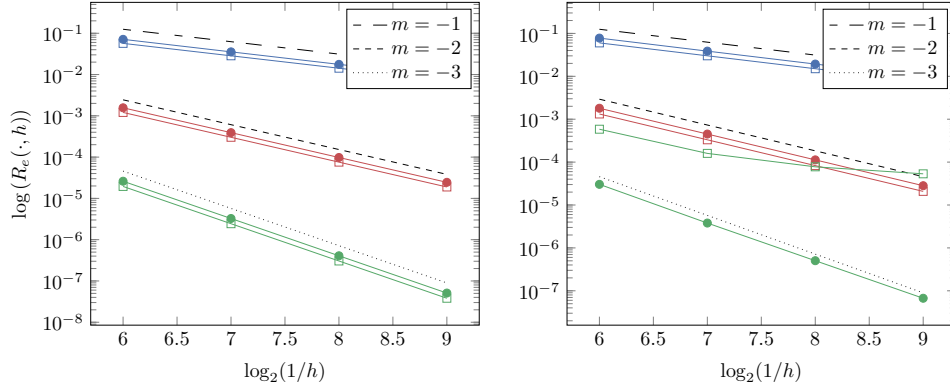


Fig. 3: Relative approximation errors and rate of convergence for the unit square domain with $c_0 = 0$, $c_1 = 1$, $\partial\Omega = \Gamma_0 \cup \Gamma_3$ and $(u, \vec{v}, \vec{\alpha}) \in DG_k(\Omega, \tau_h) \times RT_{k+1}(\Omega, \tau_h) \times RT_{k+1}(\Omega, \tau_h)$, $k = 0, 1, 2$. Blue, red, and green lines present results for $k = 0, 1, 2$, respectively. Left: smooth solution $u_{ex} = u_{1ex}$. Right: rough solution $u_{ex} = u_{2ex}$.

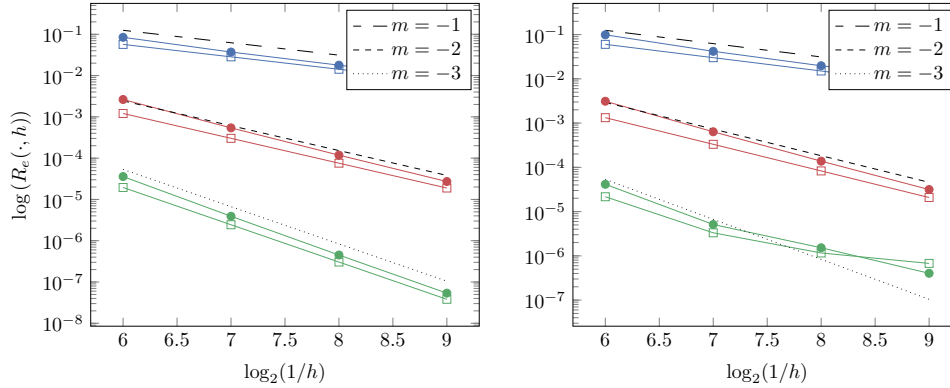


Fig. 4: Relative approximation errors and rates of convergence for the unit square domain with $c_0 = 2$, $c_1 = 4$, $\partial\Omega = \Gamma_0 \cup \Gamma_2 \cup \Gamma_3$ and $(u, \vec{v}, \vec{\alpha}) \in DG_k(\Omega, \tau_h) \times RT_{k+1}(\Omega, \tau_h) \times RT_{k+1}(\Omega, \tau_h)$, $k = 0, 1, 2$. Blue, red, and green lines present results for $k = 0, 1, 2$, respectively. Left: smooth solution $u_{ex} = u_{1ex}$. Right: rough solution $u_{ex} = u_{2ex}$.

from the analysis.

To demonstrate the effectiveness of the monolithic multigrid preconditioner, Table 2 presents iteration counts and CPU times to solution for both the multigrid-preconditioned FGMRES iterations and the use of a direct solver (MUMPS [4], via the PETSc interface) for the unit square domain with $(u, \vec{v}, \vec{\alpha}) \in DG_2(\Omega, \tau_h) \times RT_3(\Omega, \tau_h) \times RT_3(\Omega, \tau_h)$ and $\partial\Omega = \Gamma_0 \cup \Gamma_3$. We note that the iteration counts for monolithic multigrid-preconditioned FGMRES are consistent through all runs and mesh sizes, and that the scaling of wall-clock time for this approach is $\mathcal{O}(N^2)$ or better throughout. While the direct solver is slightly faster for small mesh sizes, we see worse than $\mathcal{O}(N^2)$ scaling for the wall-clock time with MUMPS at larger mesh sizes,

Table 2: Wall-clock time (in seconds) and iterations to convergence with varying numbers of processors, p , for monolithic multigrid and a direct solver (MUMPS) for the unit square domain with $c_0 = 0$, $c_1 = 1$, $\partial\Omega = \Gamma_0 \cup \Gamma_3$ and $(u, \vec{v}, \vec{\alpha}) \in DG_2(\Omega, \tau_h) \times RT_3(\Omega, \tau_h) \times RT_3(\Omega, \tau_h)$.

h^{-1}	Monolithic			MUMPS	
	Iterations	Time ($p = 1$)	Time ($p = 4$)	Time ($p = 1$)	Time ($p = 4$)
2^6	5	27.99	11.63	5.44	2.82
2^7	5	102.18	35.35	21.45	11.40
2^8	5	405.00	127.43	93.27	46.84
2^9	5	1621.38	569.88	438.91	218.88

Table 3: Wall-clock time (in seconds) and iterations to convergence with varying numbers of processors, p , for monolithic multigrid and a direct solver (MUMPS) for the unit square domain with $c_0 = 2$, $c_1 = 4$, $\partial\Omega = \Gamma_0 \cup \Gamma_2 \cup \Gamma_3$ and $(u, \vec{v}, \vec{\alpha}) \in DG_1(\Omega, \tau_h) \times RT_2(\Omega, \tau_h) \times RT_2(\Omega, \tau_h)$.

h^{-1}	Monolithic			MUMPS	
	Iterations	Time ($p = 4$)	Time ($p = 16$)	Time ($p = 4$)	Time ($p = 16$)
2^7	5	13.91	7.15	4.97	3.29
2^8	5	44.31	16.08	20.72	13.30
2^9	5	171.90	50.39	93.93	62.33
2^{10}	5	843.30	211.65	446.23	289.33

showing the expected behaviour. Moreover, as we vary the number of processors over which we parallelize the computation, we see that, for sufficiently large problems, we have good strong parallel scalability with the monolithic multigrid solver, although MUMPS is always faster than our multigrid implementation for this problem. Table 3 presents the case of $\partial\Omega = \Gamma_0 \cup \Gamma_2 \cup \Gamma_3$, $(u, \vec{v}, \vec{\alpha}) \in DG_1(\Omega, \tau_h) \times RT_2(\Omega, \tau_h) \times RT_2(\Omega, \tau_h)$. As we increase number of processors from 4 to 16, we see better performance with the multigrid solver than the direct solver. Again, we have good strong parallel scalability with the monolithic multigrid solver, showing 3.98x speedup for the 1024^2 mesh, while the direct solver (MUMPS) shows only 1.54x speedup.

We next consider the classical biharmonic problem, i.e., $c_1 = c_2 = 0$ with the exact solution u_{1ex} . Figure 5 (left) shows results for the case where $\partial\Omega = \Gamma_0 \cup \Gamma_1 \cup \Gamma_2$, and we take $(u, \vec{v}, \vec{\alpha}) \in DG_2(\Omega, \tau_h) \times RT_3(\Omega, \tau_h) \times RT_3(\Omega, \tau_h)$. For this choice ($k = 2$), Corollary 4.6 gives an expected convergence rate of $\mathcal{O}(h^2)$ for (u, \vec{v}) and of $\mathcal{O}(h^{3/2})$ for $\vec{\alpha}$. In contrast with that result, we observe almost $\mathcal{O}(h^{11/4})$ for (u, \vec{v}) in the modified $L^2 \times H(\text{div})$ norm, better than predicted, and $\mathcal{O}(h^{3/2})$ convergence for $\vec{\alpha}$, matching Corollary 4.6. Figure 5 (right) considers the L-shaped domain with $\partial\Omega = \Gamma_0$ and $k = 0, 1, 2$. Here, we observe optimal convergence rates. We note that this is a test using a manufactured solution and not a generic smooth forcing function, so the lack of full regularity from the domain is not expected to degrade the expected convergence rates.

Finally, we consider the classical biharmonic operator with clamped boundary

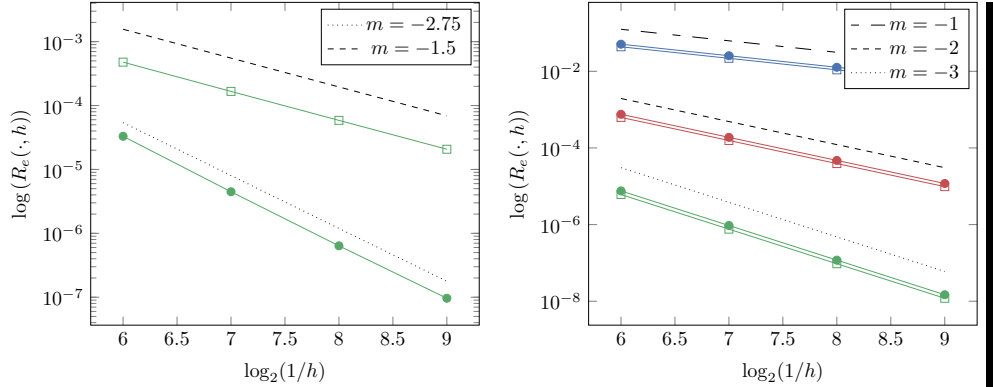


Fig. 5: Relative approximation errors and rate of convergence for the biharmonic problem in the unit square domain and $\partial\Omega = \Gamma_0 \cup \Gamma_1 \cup \Gamma_3$ (left), and the L-shaped domain with $\partial\Omega = \Gamma_0$ (right). Blue, red, and green lines present results for $k = 0, 1, 2$, respectively.

Table 4: Number of iterations to converge with different weights on the auxiliary operator. Here $(u, \vec{v}, \vec{\alpha}) \in DG_3(\Omega, \tau_h) \times RT_4(\Omega, \tau_h) \times RT_4(\Omega, \tau_h)$. A dash means that convergence was not achieved in 100 iterations.

h^{-1}	weight					
	1	10	20	40	80	h^{-1}
2^6	23	11	11	11	10	10
2^7	-	15	11	10	10	10
2^8	-	22	16	11	11	10
2^9	-	-	-	-	19	10

conditions, i.e., $c_0 = c_1 = 0$ and $\partial\Omega = \Gamma_1$ and $(u, \vec{v}, \vec{\alpha}) \in DG_3(\Omega, \tau_h) \times RT_4(\Omega, \tau_h) \times RT_4(\Omega, \tau_h)$. Table 4 shows the effectiveness of the monolithic multigrid solver with an $\mathcal{O}(h^{-1})$ weight on the auxiliary operator. Dashes in the table mean that more than a hundred iterations are required to converge when the residual norm or its relative reduction is less than 10^{-12} . We note that, due to a technical limitation in PCPATCH (where Nitsche boundary terms cannot be treated), these results use an alternate implementation of the star relaxation scheme that is less efficient than PCPATCH. Consequently, we do not report timings for these experiments, as they are not comparable to the timings reported elsewhere in this paper.

6.2. 3D experiments. Here, we consider a test case on the unit cube, with right-hand side and boundary conditions chosen so that the exact solution is $u_{ex} = \sin(2\pi x) \cos(3\pi y) \sinh(\pi z)$. Finite-element convergence is demonstrated in Figure 6 for $k \in \{0, 1, 2\}$ with $\partial\Omega = \Gamma_0 \cup \Gamma_2 \cup \Gamma_3$, with Γ_0 corresponding to $z = 0$ and $z = 1$, Γ_2 corresponding to $y = 0$ and $y = 1$, and Γ_3 corresponding to $x = 0$ and $x = 1$, showing convergence consistent with the analysis of Theorem 4.4. Table 5 details the performance of the monolithic multigrid-preconditioned FGMRES solver for $k = 0$, compared with a standard direct solver (MUMPS). We see excellent performance

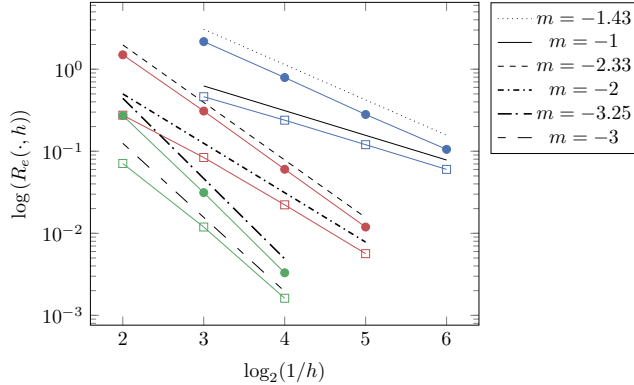


Fig. 6: Relative approximation errors and rates of convergence for the unit cube domain $\partial\Omega = \Gamma_0 \cup \Gamma_2 \cup \Gamma_3$, $c_0 = 4$ and $c_1 = 2$. Blue, red, and green lines present results for $k = 0, 1, 2$, respectively.

Table 5: Wall-clock time (in seconds) and iterations to convergence with varying numbers of processors, p , for monolithic multigrid and a direct solver (MUMPS) for the unit cube domain with $c_0 = 4$, $c_1 = 2$, $\partial\Omega = \Gamma_0 \cup \Gamma_2 \cup \Gamma_3$ and $(u, \vec{v}, \vec{\alpha}) \in DG_0(\Omega, \tau_h) \times RT_1(\Omega, \tau_h) \times RT_1(\Omega, \tau_h)$.

h^{-1}	Monolithic			MUMPS	
	Iterations	Time ($p = 1$)	Time ($p = 8$)	Time ($p = 1$)	Time ($p = 8$)
2^3	9	5.55	2.80	1.51	0.69
2^4	9	31.10	7.30	11.05	3.75
2^5	9	229.65	38.31	154.33	44.07
2^6	9	1847.65	280.42	5173.58	1167.10

of the monolithic multigrid method, with iteration counts that are independent of problem size and CPU time scaling linearly with problem size, and decreasing with parallelization for sufficiently large problems. In contrast, we see the expected rapid growth of required CPU times for MUMPS, and suboptimal parallel scaling, showing the utility and power of the monolithic multigrid approach.

7. Conclusion. We consider the mixed finite-element approximation of solutions to modified biharmonic problems, achieved by the transformation of the fourth-order equation into a system of PDEs. We find that under natural assumptions on the coefficients of the problem, three combinations of boundary conditions lead to optimal finite-element convergence. For the fourth case of boundary conditions (on the solution and its normal derivative), suboptimal rates of convergence are expected and observed when implemented using Nitsche’s method. While the approach is applicable in both two and three dimensions, we note that it is particularly attractive in 3D, where the cost of conforming methods is prohibitive.

It remains an open question whether or not it is possible to employ alternative approaches (such as adapting the Nitsche boundary conditions, or the use of alternative penalty approaches) to regain optimal finite-element convergence for the boundary

conditions where suboptimal convergence is proven and observed here.

We additionally propose an monolithic multigrid algorithm with optimal scaling for the resulting discrete linear systems. For three-dimensional problems, this approach yields a preconditioned FGMRES iteration that dramatically outperforms standard direct solvers.

REFERENCES

- [1] J. H. ADLER, T. J. ATHERTON, T. R. BENSON, D. B. EMERSON, AND S. P. MACLACHLAN, *Energy minimization for liquid crystal equilibrium with electric and flexoelectric effects*, SIAM J. Sci. Comput., 37 (2015), pp. S157–S176, <https://doi.org/10.1137/140975036>.
- [2] J. H. ADLER, T. BENSON, E. C. CYR, P. E. FARRELL, S. MACLACHLAN, AND R. TUMINARO, *Monolithic multigrid for magnetohydrodynamics*, SIAM J. Sci. Comput., (2021), pp. S70–S91, <https://doi.org/10.1137/20M1348364>.
- [3] J. H. ADLER, T. R. BENSON, AND S. P. MACLACHLAN, *Preconditioning a mass-conserving discontinuous Galerkin discretization of the Stokes equations*, Numer. Linear Algebra Appl., 24 (2017), pp. e2047, 23, <https://doi.org/10.1002/nla.2047>.
- [4] P. R. AMESTOY, I. S. DUFF, J. KOSTER, AND J.-Y. L’EXCELLENT, *A fully asynchronous multi-frontal solver using distributed dynamic scheduling*, SIAM J. Matrix Anal. Appl., 23 (2001), pp. 15–41.
- [5] D. ARNOLD, R. FALK, AND R. WINTHER, *Multigrid in $H(\text{div})$ and $H(\text{curl})$* , Numer. Math., 85 (2000), pp. 197–217.
- [6] D. N. ARNOLD, R. S. FALK, AND J. GOPALAKRISHNAN, *Mixed finite element approximation of the vector Laplacian with Dirichlet boundary conditions*, Math. Models Methods Appl. Sci., 22 (2012), pp. 1250024, 26, <https://doi.org/10.1142/S0218202512500248>.
- [7] D. N. ARNOLD, R. S. FALK, AND R. WINTHER, *Preconditioning in $H(\text{div})$ and applications*, Math. Comp., 66 (1997), pp. 957–984, <https://doi.org/10.1090/S0025-5718-97-00826-0>.
- [8] J.-P. AUBIN, *Approximation of elliptic boundary-value problems*, Wiley-Interscience [A division of John Wiley & Sons, Inc.], New York-London-Sydney, 1972. Pure and Applied Mathematics, Vol. XXVI.
- [9] I. BABUŠKA, *The finite element method with penalty*, Math. Comp., 27 (1973), pp. 221–228, <https://doi.org/10.2307/2005611>.
- [10] I. BABUŠKA AND M. ZLÁMAL, *Nonconforming elements in the finite element method with penalty*, SIAM J. Numer. Anal., 10 (1973), pp. 863–875, <https://doi.org/10.1137/0710071>.
- [11] G. A. BAKER, *Finite element methods for elliptic equations using nonconforming elements*, Math. Comp., 31 (1977), pp. 45–59, <https://doi.org/10.2307/2005779>.
- [12] S. BALAY, S. ABHYANKAR, M. ADAMS, J. BROWN, P. BRUNE, K. BUSCHELMAN, L. DALCIN, A. DENER, V. ELJKHOUT, W. GROPP, ET AL., *PETSc users manual: Revision 3.10*, tech. report, Argonne National Lab.(ANL), Argonne, IL (United States), 2018.
- [13] L. BANZ, B. P. LAMICHHANE, AND E. P. STEPHAN, *A new three-field formulation of the biharmonic problem and its finite element discretization*, Numer. Methods Partial Differential Equations, 33 (2017), pp. 199–217, <https://doi.org/10.1002/num.22082>.
- [14] L. BANZ, J. PETSCHKE, AND A. SCHRÖDER, *Two stabilized three-field formulations for the biharmonic problem*, in Chemnitz Finite Element Symposium, Springer, 2017, pp. 41–55.
- [15] E. M. BEHRENS AND J. GUZMÁN, *A mixed method for the biharmonic problem based on a system of first-order equations*, SIAM J. Numer. Anal., 49 (2011), pp. 789–817, <https://doi.org/10.1137/090775245>.
- [16] J. BENZAKEN, J. A. EVANS, S. F. MCCORMICK, AND R. TAMSTORF, *Nitsche’s method for linear Kirchhoff–Love shells: Formulation, error analysis, and verification*, Comput. Methods Appl. Mech. Engrg., 374 (2021), p. 113544, <https://doi.org/https://doi.org/10.1016/j.cma.2020.113544>.
- [17] M. BENZI, G. H. GOLUB, AND J. LIESEN, *Numerical solution of saddle point problems*, Acta Numer., 14 (2005), pp. 1–137, <https://doi.org/10.1017/S0962492904000212>.
- [18] D. BOFFI, F. BREZZI, AND M. FORTIN, *Mixed finite element methods and applications*, vol. 44 of Springer Series in Computational Mathematics, Springer, Heidelberg, 2013, <https://doi.org/10.1007/978-3-642-36519-5>.
- [19] D. BRAESS, *Finite elements*, Cambridge University Press, Cambridge, third ed., 2007, <https://doi.org/10.1017/CBO9780511618635>. Theory, fast solvers, and applications in elasticity theory, Translated from the German by Larry L. Schumaker.
- [20] S. C. BRENNER, S. GU, T. GUDI, AND L.-Y. SUNG, *A quadratic C^0 interior penalty method for*

- linear fourth order boundary value problems with boundary conditions of the Cahn-Hilliard type, *SIAM J. Numer. Anal.*, 50 (2012), pp. 2088–2110, <https://doi.org/10.1137/110847469>.
- [21] S. C. BRENNER AND L. R. SCOTT, *The mathematical theory of finite element methods*, vol. 15 of Texts in Applied Mathematics, Springer, New York, third ed., 2008, <https://doi.org/10.1007/978-0-387-75934-0>.
- [22] S. C. BRENNER AND L.-Y. SUNG, C^0 interior penalty methods for fourth order elliptic boundary value problems on polygonal domains, *J. Sci. Comput.*, 22/23 (2005), pp. 83–118, <https://doi.org/10.1007/s10915-004-4135-7>.
- [23] X.-L. CHENG, W. HAN, AND H.-C. HUANG, *Some mixed finite element methods for biharmonic equation*, *J. Comput. Appl. Math.*, 126 (2000), pp. 91–109, [https://doi.org/10.1016/S0377-0427\(99\)00342-8](https://doi.org/10.1016/S0377-0427(99)00342-8).
- [24] P. G. CIARLET, *The finite element method for elliptic problems*, North-Holland Publishing Co., Amsterdam-New York-Oxford, 1978. Studies in Mathematics and its Applications, Vol. 4.
- [25] H. C. ELMAN, D. J. SILVESTER, AND A. J. WATHEN, *Finite elements and fast iterative solvers: with applications in incompressible fluid dynamics*, Numerical Mathematics and Scientific Computation, Oxford University Press, New York, 2005.
- [26] A. EMBAR, J. DOLBOW, AND I. HARARI, *Imposing Dirichlet boundary conditions with Nitsche’s method and spline-based finite elements*, *Int. J. Numer. Methods Engrg.*, 83 (2010), pp. 877–898, <https://doi.org/10.1002/nme.2863>.
- [27] G. ENGEL, K. GARikipATI, T. J. R. HUGHES, M. G. LARSON, L. MAZZEI, AND R. L. TAYLOR, *Continuous/discontinuous finite element approximations of fourth-order elliptic problems in structural and continuum mechanics with applications to thin beams and plates, and strain gradient elasticity*, *Comput. Methods Appl. Mech. Engrg.*, 191 (2002), pp. 3669–3750, [https://doi.org/10.1016/S0045-7825\(02\)00286-4](https://doi.org/10.1016/S0045-7825(02)00286-4).
- [28] P. E. FARRELL, M. G. KNEPLEY, F. WECHSUNG, AND L. MITCHELL, *PCPATCH: software for the topological construction of multigrid relaxation methods*, *ACM Transactions on Mathematical Software*, (2021), <https://arxiv.org/abs/1912.08516>. In press.
- [29] P. E. FARRELL, L. MITCHELL, AND F. WECHSUNG, *An Augmented Lagrangian Preconditioner for the 3D Stationary Incompressible Navier–Stokes Equations at High Reynolds Number*, *SIAM J. Sci. Comput.*, 41 (2019), pp. A3073–A3096, <https://doi.org/10.1137/18M1219370>.
- [30] J. FREUND AND R. STENBERG, *On weakly imposed boundary conditions for second order problems*, *Proceedings of the Ninth International Conference on Finite Elements in Fluids*, (1995), pp. 327–336.
- [31] V. GIRAULT AND P.-A. RAVIART, *Finite element methods for Navier-Stokes equations: Theory and algorithms*, vol. 5 of Springer Series in Computational Mathematics, Springer-Verlag, Berlin, 1986, <https://doi.org/10.1007/978-3-642-61623-5>.
- [32] P. GRISVARD, *Elliptic problems in nonsmooth domains*, vol. 69 of Classics in Applied Mathematics, Society for Industrial and Applied Mathematics (SIAM), Philadelphia, PA, 2011, <https://doi.org/10.1137/1.9781611972030.ch1>.
- [33] M. ILYAS AND B. LAMICHHANE, *A three-field formulation of the Poisson problem with Nitsche approach*, *ANZIAM Journal*, 59 (2017), <https://doi.org/10.21914/anziamj.v59i0.12645>.
- [34] C. JOHNSON AND J. PITKÄRANTA, *Analysis of some mixed finite element methods related to reduced integration*, *Math. Comp.*, 38 (1982), pp. 375–400, <https://doi.org/10.2307/2007276>.
- [35] M. JUNTUNEN AND R. STENBERG, *Nitsche’s method for general boundary conditions*, *Math. Comp.*, 78 (2009), pp. 1353–1374, <https://doi.org/10.1090/S0025-5718-08-02183-2>.
- [36] R. KIRBY AND L. MITCHELL, *Code generation for generally mapped finite elements*, *ACM Trans. Math. Software*, 45 (2019), pp. 1–23, <https://doi.org/10.1145/3361745>.
- [37] R. C. KIRBY, *From functional analysis to iterative methods*, *SIAM Rev.*, 52 (2010), pp. 269–293, <https://doi.org/10.1137/070706914>.
- [38] R. C. KIRBY, A. LOGG, M. E. ROGNES, AND A. R. TERREL, *Common and unusual finite elements*, in *Automated Solution of Differential Equations by the Finite Element Method*, Springer, 2012, pp. 95–119.
- [39] R. C. KIRBY AND L. MITCHELL, *Solver composition across the PDE/linear algebra barrier*, *SIAM J. Sci. Comput.*, 40 (2018), pp. C76–C98.
- [40] Z. LI AND S. ZHANG, *A stable mixed element method for the biharmonic equation with first-order function spaces*, *Comput. Methods Appl. Math.*, 17 (2017), pp. 601–616, <https://doi.org/10.1515/cmam-2017-0002>.
- [41] S. P. MACLACHLAN AND C. W. OOSTERLEE, *Local Fourier analysis for multigrid with overlapping smoothers applied to systems of PDEs*, *Numer. Linear Algebra Appl.*, 18 (2011), pp. 751–774, <https://doi.org/10.1002/nla.762>.
- [42] D. S. MALKUS AND T. J. HUGHES, *Mixed finite element methods, reduced and selective integration techniques: a unification of concepts*, *Comput. Meth. Appl. Mech. Eng.*, 15 (1978),

- pp. 63–81.
- [43] K.-A. MARDAL AND R. WINTHER, *Preconditioning discretizations of systems of partial differential equations*, Numer. Lin. Alg. Appl., 18 (2011), pp. 1–40, <https://doi.org/10.1002/nla.716>.
 - [44] P. MONK, *A mixed finite element method for the biharmonic equation*, SIAM J. Numer. Anal., 24 (1987), pp. 737–749, <https://doi.org/10.1137/0724048>.
 - [45] M. F. MURPHY, G. H. GOLUB, AND A. J. WATHEN, *A note on preconditioning for indefinite linear systems*, SIAM J. Sci. Comput., 21 (2000), pp. 1969–1972, <https://doi.org/10.1137/S1064827599355153>.
 - [46] A. NATALE, J. SHIPTON, AND C. J. COTTER, *Compatible finite element spaces for geophysical fluid dynamics*, Dynamics and Statistics of the Climate System, 1 (2016), <https://doi.org/10.1093/climsys/dzw005>.
 - [47] T. D. NGUYEN, *Discontinuous Galerkin formulations for thin bending problems*, PhD thesis, Delft University of Technology, 2008.
 - [48] J. NITSCHKE, *Über ein Variationsprinzip zur Lösung von Dirichlet-Problemen bei Verwendung von Teilräumen, die keinen Randbedingungen unterworfen sind*, Abhandlungen aus dem Mathematischen Seminar der Universität Hamburg, 36 (1971), pp. 9–15, <https://doi.org/10.1007/bf02995904>.
 - [49] M. Y. PEVNYI, J. V. SELINGER, AND T. J. SLUCKIN, *Modeling smectic layers in confined geometries: Order parameter and defects*, Phys. Rev. E, 90 (2014), p. 032507.
 - [50] F. RATHGEBER, D. A. HAM, L. MITCHELL, M. LANGE, F. LUPORINI, A. T. MCRAE, G.-T. BERCEA, G. R. MARKALL, AND P. H. KELLY, *Firedrake: automating the finite element method by composing abstractions*, ACM Trans. Math. Software, 43 (2017), p. 24.
 - [51] B. RIVIÈRE, *Discontinuous Galerkin methods for solving elliptic and parabolic equations: Theory and implementation*, vol. 35 of Frontiers in Applied Mathematics, Society for Industrial and Applied Mathematics (SIAM), Philadelphia, PA, 2008, <https://doi.org/10.1137/1.9780898717440>.
 - [52] Y. SAAD, *A flexible inner-outer preconditioned GMRES algorithm*, SIAM J. Sci. Comput., 14 (1993), pp. 461–469, <https://doi.org/10.1137/0914028>.
 - [53] S. P. VANKA, *Block-implicit multigrid solution of Navier-Stokes equations in primitive variables*, J. Comput. Phys., 65 (1986), pp. 138–158, [https://doi.org/10.1016/0021-9991\(86\)90008-2](https://doi.org/10.1016/0021-9991(86)90008-2).
 - [54] M. WANG AND J. XU, *The Morley element for fourth order elliptic equations in any dimensions*, Numer. Math., 103 (2006), pp. 155–169, <https://doi.org/10.1007/s00211-005-0662-x>.
 - [55] P. WANG, L. JIANG, AND S. CHEN, *A nonconforming scheme for non-Fickian flow in porous media*, J. Inequal. Appl., (2017), pp. Paper No. 142, 16, <https://doi.org/10.1186/s13660-017-1419-7>.
 - [56] T. WARBURTON AND J. S. HESTHAVEN, *On the constants in hp-finite element trace inverse inequalities*, Comput. Methods Appl. Mech. Engrg., 192 (2003), pp. 2765–2773, [https://doi.org/10.1016/S0045-7825\(03\)00294-9](https://doi.org/10.1016/S0045-7825(03)00294-9).
 - [57] *Software used in ‘A new mixed finite-element method for the biharmonic problem’*, may 2021, <https://doi.org/10.5281/zenodo.4749355>, <https://doi.org/10.5281/zenodo.4749355>.